N-1816

NCEL

Technical Note

October 1990

By Jack W. DeVries

Sponsored By Office of the Chief of Naval Research

FIELD MEASUREMENTS OF ESTUARIAL COHESIVE SEDIMENT TRANSPORT

ABSTRACT Predictive modeling of estuarial fine sediment transport requires a description of the erosional properties of cohesive sediment beds. Available descriptions are commonly based upon flume experiments run on remolded beds. Field data pertaining to the laboratory erosion process are particularly scarce, thus it is unknown how well these estimates relate to the actual erosion process. A field experiment was conducted in a muddy estuary, Mare Island Strait, California, to address these issues. Using a bottom-mounted frame and a moveable instrument sled, suspended sediment concentration and current velocity data were collected in the bottom boundary layer. The critical shear stress of erosion initiation and the erosion rate coefficient were determined from these data. It was found that flume experiments using naturally deposited sediment beds do a reasonable job in predicting both of these parameters, but that experiments using remolded sediments do not approximate the conditions encountered in the field.

NAVAL CIVIL ENGINEERING LABORATORY PORT HUENEME CALIFORNIA 93043-5003

METRIC CONVERSION FACTORS

Approximate Conversions to Metric Measures

Symbol	When You Know	Multiply by	To Find	Symbol
		LENGTH		
in	inches	*2.5	centimeters	cm
ft	feet	30	centimeters	cm
yd	yards	0.9	meters	m
mi	miles	1.6	kilometers	km
		AREA		
in^2	square inches	6.5	square centimeters	cm^2
ft^2	square feet	0.09	square meters	m^2
yd^2	square yards	0.8	square meters	m^2
mi^2	square miles	2.6	square kilometers	km^2
	acres	0.4	hectares	ha
		MASS (weight)		
oz	ounces	28	grams	g
lb	pounds	0.45	kilograms	kg
	short tons (2,000 lb)	0.9	tonnes	t
		VOLUME		
tsp	teaspoons	5	milliliters	ml
Tbsp	tablespoons	15	milliliters	ml
fl oz	fluid ounces	30	milliliters	ml
c	cups	0.24	liters	l
pt	pints	0.47	liters	l
qt	quarts	0.95	liters	l
gal	gallons	3.8	liters	l
ft^3	cubic feet	0.03	cubic meters	m^3
yd^3	cubic yards	0.76	cubic meters	m^3
		TEMPERATURE (exact)		
°F	Fahrenheit temperature	5/9 (after subtracting 32)	Celsius temperature	°C

*1 in = 2.54 (exactly). For other exact conversions and more detailed tables, see NBS Misc. Publ. 286, Units of Weights and Measures, Price $2.25, SD Catalog No. C13.10:286.

Approximate Conversions from Metric Measures

Symbol	When You Know	Multiply by	To Find	Symbol
		LENGTH		
mm	millimeters	0.04	inches	in
cm	centimeters	0.4	inches	in
m	meters	3.3	feet	ft
m	meters	1.1	yards	yd
km	kilometers	0.6	miles	mi
		AREA		
cm^2	square centimeters	0.16	square inches	in^2
m^2	square meters	1.2	square yards	yd^2
km^2	square kilometers	0.4	square miles	mi^2
ha	hectares (10,000 m^2)	2.5	acres	
		MASS (weight)		
g	grams	0.035	ounces	oz
kg	kilograms	2.2	pounds	lb
t	tonnes (1,000 kg)	1.1	short tons	
		VOLUME		
ml	milliliters	0.03	fluid ounces	fl oz
l	liters	2.1	pints	pt
l	liters	1.06	quarts	qt
l	liters	0.26	gallons	gal
m^3	cubic meters	35	cubic feet	ft^3
m^3	cubic meters	1.3	cubic yards	yd^3
		TEMPERATURE (exact)		
°C	Celsius temperature	9/5 (then add 32)	Fahrenheit temperature	°F

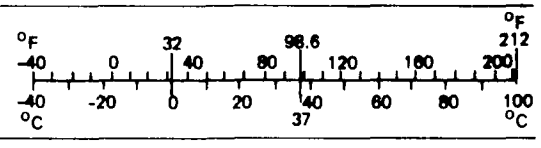

REPORT DOCUMENTATION PAGE

Form Approved
OMB No. 0704-018

1. AGENCY USE ONLY *(Leave blank)*	2. REPORT DATE	3. REPORT TYPE AND DATES COVERED
	October 1990	Final: Oct 86 through Sep 88

4. TITLE AND SUBTITLE

FIELD MEASUREMENTS OF ESTUARIAL COHESIVE SEDIMENT TRANSPORT

5. FUNDING NUMBERS

PE - 61152N
PR - R000-NO-200
WU - DN668058

6. AUTHOR(S)

Jack W. DeVries

7. PERFORMING ORGANIZATION NAME(S) AND ADDRESSE(S)

Naval Civil Engineering Laboratory
Port Hueneme, CA 93043-5003

8. PERFORMING ORGANIZATION REPORT NUMBER

TN - 1816

9. SPONSORING/MONITORING AGENCY NAME(S) AND ADDRESSE(S)

Office of the Chief of Naval Research
Office of Naval Research
Arlington, VA 22217-5000

10. SPONSORING/MONITORING AGENCY REPORT NUMBER

11. SUPPLEMENTARY NOTES

12a. DISTRIBUTION/AVAILABILITY STATEMENT

Approved for public release; distribution unlimited.

12b. DISTRIBUTION CODE

13. ABSTRACT *(Maximum 200 words)*

Predictive modeling of estuarial fine sediment transport requires a description of the erosional properties of cohesive sediment beds. Available descriptions are commonly based upon flume experiments run on remolded beds. Field data pertaining to the laboratory erosion process are particularly scarce, thus it is unknown how well these estimates relate to the actual erosion process. A field experiment was conducted in a muddy estuary, Mare Island Strait, California, to address these issues. Using a bottom-mounted frame and a moveable instrument sled, suspended sediment concentration and current velocity data were collected in the bottom boundary layer. The critical shear stress of erosion initiation and the erosion rate coefficient were determined from these data. It was found that flume experiments using naturally deposited sediment beds do a reasonable job in predicting both of these parameters, but that experiments using remolded sediments do not approximate the conditions encountered in the field.

14. SUBJECT TERMS

Sediment transport, cohesive, mud, clay, sedimentation, harbors, shoaling

15. NUMBER OF PAGES

65

16. PRICE CODE

17. SECURITY CLASSIFICATION OF REPORT	18. SECURITY CLASSIFICATION OF THIS PAGE	19. SECURITY CLASSIFICATION OF ABSTRACT	20. LIMITATION OF ABSTRACT
Unclassified	Unclassified	Unclassified	UL

CONTENTS

INTRODUCTION

Many Navy berths that are located in estuaries dominated by cohesive sediments are plagued by sedimentation. Presently, cutter-suction dredges are used to maintain operable depths in these berths. However, the inconvenience of these dredges and the ever-increasing costs associated with dredging and dredge spoil disposal have prompted the Navy to consider the development of efficient sediment management plans for each problem harbor. These plans would include sediment resuspension systems, sediment exclusion systems, and an optimized dredging schedule. To initiate these solutions, it is necessary to have a rational means of analyzing the sediment transport problems that currently exist in each harbor as well as a means of predicting how the sediment transport might vary with future harbor developments.

Most available predictive models of estuarial fine-sediment transport are based upon theoretical formulations supported by laboratory flume experiments. Since field data pertaining to these transport processes are particularly scarce, it is unknown how well these laboratory estimates relate to the actual process.

This work was funded through the Independent Research Program at the Naval Civil Engineering Laboratory (NCEL) by the Office of Naval Research (ONR).

OBJECTIVE

The commonly used models for erosion, deposition, and transportation of suspended sediments will be reviewed. Many of these models require parameters that are either poorly understood or difficult to quantify. The objective of this study is to investigate the true character of these parameters for one estuarine environment, and to use this information as a basis from which to comment on the appropriateness of the estimation methods currently available for cohesive sediment transport modeling.

APPROACH

A field experiment was undertaken to gather the data necessary to address the quantitative validity of the most popular methods for predicting cohesive sediment transport.

BACKGROUND

There are three processes involved in estuarial cohesive sediment transport: (1) the erosion of the sediment bed, (2) the deposition of suspended sediment onto the bed, and (3) the transportation of suspended

sediments laterally through the water column. Each of these processes has to be modeled in a reasonable fashion in order to predict the shoaling characteristics of a harbor.

Erosion

The process of erosion involves the resuspension of material from the sediment bed. This can occur either as surface erosion, where one particle at a time is removed, or as bulk erosion, where large masses of sediment are resuspended at once. In quasi-steady flow environments, surface erosion typically dominates. There is a wide diversity of equations that have been used to describe the rate of surface erosion (Mehta, et al., 1982). Of these, the formulation presented by Partheniades (1962) is the most common:

$$E = M \left(\frac{\tau_b - \tau_c}{\tau_c} \right) \qquad (1)$$

where: E = rate of surface erosion

M = erosion rate coefficient

τ_b = bed shear stress

τ_c = critical shear stress

Two of the three parameters in Equation 1, the erosion rate coefficient and the critical shear stress, are not well understood.

A few attempts have been made to quantify the erosion rate coefficient, M. The estimates of M resulting from these investigations vary by two orders of magnitude. Ariathurai and Arulanandan (1978) placed remolded cylindrical samples of differing sediment types and pore fluid compositions into a bath of eroding fluid. They found that the erosion rate coefficient varied from 3 to 30 milligrams/square centimeter-minute. The value of the coefficient was most significantly affected by the cation exchange capacity (a measure of the soil chemistry) and the sodium absorption ratio (a measure of the water chemistry). More recently Ockenden and Delo (1988) conducted a series of flume experiments to determine the erosion rate coefficient. Using an annular flume, they imposed a uniform bed shear stress upon a naturally deposited sediment bed. Based on these experiments they suggest that the erosion rate coefficient is a function of the proportion of sand within the sediment (a sieved natural sediment was used). Values ranged from 0.36 milligrams/square centimeter-minute for 0 percent sand to 0.06 milligrams/square centimeter-minute for 11 percent sand.

The critical shear stress is a rather nebulous term that addresses the strength properties of the sediment bed. Parchure and Mehta (1985) have shown that this value is not constant, but varies with depth into the sediment bed. Based on laboratory tests, they suggest that this variation lends itself to a three-zoned description (see Figure 1).

Each of these zones is defined by a reference shear strength: the upper zone is defined by the shear strength at the sediment bed surface ($z = 0$), τ_{so}, which is the critical shear stress of erosion initiation; the middle zone is defined by the shear strength at the point of greatest curvature of the shear strength versus depth curve, τ_{sc}; and the lowest zone is marked by the maximum shear strength, τ_{sm}. The range of values obtained for redeposited clay in the laboratory for each of these shear strengths is listed in Table 1.

Deposition

The process of deposition involves the settling of particle aggregates from the water column. These aggregates adhere, in whole or in part, to the sediment bed. Krone (1962) describes this process as follows:

$$\frac{dc}{dt} = -\left(\frac{cW_s P}{y}\right) \qquad (2)$$

where: dc/dt = deposition rate (time rate of change of the suspended sediment concentration)

c = suspended sediment concentration

W_s = aggregate settling velocity

P = probability of a particle sticking to the bed

y = water depth

The probability of a particle sticking to the bed is defined as:

$$P = 1 - \left(\frac{\tau_w}{\tau_{cd}}\right) \qquad (3)$$

where: τ_w = bed shear stress

τ_{cd} = critical shear stress of deposition ($\tau_{cd} \leq \tau_w$)

As with the erosion process, the critical shear stress parameter for the deposition process is not well understood. The critical shear stress of deposition is defined as the shear stress below which all suspended sediment eventually deposits. Its value has been estimated by conducting laboratory flume experiments using sediments sampled from various locations. The differences in these values may be related to grain characteristics, but no generally accepted relationship is available. Table 2 lists these values.

Transportation

The process of transportation involves the lateral movement of the suspended sediment load through the water column; this process can alternately be defined as the mass flux of sediment through discrete control volumes within the estuary (see Figure 2). The mass flux, F, through a discrete surface is defined as:

$$F = \oint_S c\,\bar{V} \cdot \bar{n}\, dS \qquad (4)$$

where: c = suspended sediment concentration

$\bar{V}$ = horizontal fluid velocity vector

$\bar{n}$ = unit vector normal to dS

dS = incremental area on the surface, S

By assuming two-dimensional flow and using vertical distributions for both the suspended sediment concentration and the horizontal fluid velocity, one reduces the above equation to:

$$F = \int_0^h C\bar{V}\, dz \qquad (5)$$

where: C = vertical distribution of the suspended sediment concentration

$\bar{V}$ = vertical distribution of the horizontal fluid velocity

dz = incremental depth

h = total depth of water

The vertical distribution of the suspended sediment concentration is normally defined by the Rouse equation (Rouse, 1938) as:

$$\frac{C}{C_o} = \left[\left(\frac{h-z}{z}\right) \left(\frac{a}{h-a}\right) \right]^{W_s/kU_*} \qquad (6)$$

where: C = suspended sediment concentration at a height, z, above the sediment bed

C_o = reference concentration at a height, a, above the sediment bed

h = total depth

z = height above the sediment bed

a = height above the bed of the reference concentration

W_s = settling velocity

k = Von Karman's constant

U_* = friction velocity

This formulation requires that a reference concentration be specified for each point at which the mass flux is required. Since it would not be practical to measure these values for a predictive model, some attempts at developing a theoretical basis have been published (Adams and Weatherly, 1981; Shi, et al., 1985). In a recent field study however, Sternberg, et al. (1986) indicated that these predictions of the reference concentration were not accurate enough to use in mass flux estimates.

The other parameter in Equation 6 that is not well understood is the settling velocity. In most modeling it is taken to be a constant, yet tests show that it can vary by as much as three orders of magnitude within the same estuary (van Leussen, 1988) (see Figure 3).

The vertical distribution of the fluid velocity is defined by the turbulent boundary layer equation for flow over a flat plate:

$$\frac{U}{U_*} = k^{-1} \ln \left(\frac{z}{z_o}\right) \qquad (7)$$

where: U = mean velocity at height, z, above the sediment bed

U_* = friction velocity

k = Von Karman's constant

z = height above the sediment bed

z_o = bed roughness height

The friction velocity is defined as:

$$U_* = \left(\frac{\tau_o}{\rho}\right)^{1/2} \qquad (8)$$

where: τ_o = bed shear stress

ρ = fluid density

Von Karman's constant for a homogeneous fluid is 0.4. It has been shown that this value varies in flows in which there is a density gradient (Vanoni and Nomicos, 1959). It is not certain what effect a suspended sediment induced density gradient would have on this constant. Adams

and Weatherly (1981) and Sternberg, et al. (1986) have used a Richardson damping scheme to simulate the effects of stratified flow, but there is little experimental verification for this approach.

FIELD EXPERIMENT

A field experiment was conducted by the Naval Civil Engineering Laboratory (NCEL) from 23 to 25 September, 1987. Suspended sediment concentration and current velocity data were collected in the bottom boundary layer of an estuarine tidal channel over a duration of five tidal cycles. These data were used in an attempt to evaluate the parameters of interest in the above-mentioned equations.

Site

The field study was conducted in Mare Island Strait, an estuarine tidal channel that acts as the principal effluence of the Napa River into the northeastern corner of the San Francisco Bay complex. The normal tidal flux within this narrow estuary greatly exceeds the freshwater effluence throughout most of the year. Tide data are shown in Figure 4. The surface wave activity within the strait is negligible, and the tide-generated current is the predominant driving force for sediment motion. The depth in a 250-meter-wide channel and in numerous shipyard berthing areas is maintained at 10.8 meters below the mean lower low-water level by a year-round dredging effort. The sediment at Mare Island consists of 46 percent silt, 42 percent clay, and 12 percent sand (Malloy, 1980). Roughly 2.5 million cubic meters of this sediment is removed annually.

System

A sliding instrumented sting, mounted upon a bottom-landing framework, was lowered onto a flat portion of the artificially-deepened channel approximately 70 feet off the quay wall that forms the western boundary of the waterway (Figure 5). This sting was oriented perpendicular to the channel axis so as to hold the instruments in an environment of unobstructed flow (Figure 6). By moving the sliding sting in the vertical plane, via a hydraulic cylinder, it was possible to use a relatively small number of instruments to profile the bottom boundary layer of the estuary. Instruments were mounted on the sting and used as follows:

- Two Marsh McBirney electromagnetic current meters (1-1/2-inch ball) were used to measure the horizontal velocity vectors in the water column.

- Five optical backscatterance sensors were used to determine the suspended sediment concentration in the water column.

- A Benthos plankton camera was used to determine the vertical distribution of floc sizes in the water column. Problems were encountered with the operation of the device, therefore no data were obtained.

- A bottom sensor, based on the design presented by Krone (1972), was employed to reference the above-mentioned measurements to the location of the bottom.

- A differential pressure transducer was used to measure the excursion of the sliding sting relative to its highest point of excursion (a fixed point on the framework).

Technique

Vertical profiles of the fluid and sediment parameters were taken at half-hour intervals during the time that the system was monitored manually. The profiling was performed in the following manner: The sting was moved downward until the bottom sensor indicated that the sediment bed had been reached. In this position the differential pressure sensor was zeroed and the first set of readings was taken. The sting was moved up to the next station and a new set of readings was taken. Figure 7 shows the positions of the stations at which the readings were taken.

Each profile (consisting of ten stations) required about 3 minutes to complete. It was assumed that steady fluid flow conditions existed during this time. To insure that this was the case, readings were taken as the sting moved both upward and downward. The results were compared, and no appreciable offset was seen in any of the profile data thereby suggesting that the assumption was valid.

In addition to the profile data, a time series of data was taken every 10 minutes at one vertical station (with the bottom sensor located 5 centimeters above the bed) for the duration of the experiment.

RESULTS

Velocity Data

Current velocity data were collected by two, two-axis electromagnetic current meters mounted in a vertical stack. These sensors were calibrated for unidirectional flow using a tow channel. In an attempt to reduce any data scatter that might have been caused by small-scale turbulence, each data point that was recorded was an average of ten measured points taken over an interval of 3 seconds. The horizontal velocity vector for each position was calculated as follows:

$$|u| = (u^2 + v^2)^{1/2} \quad , \quad \theta = \tan^{-1}\left(\frac{v}{u}\right) \tag{9}$$

where: $|u|$ = magnitude of the velocity vector

u = current velocity along the channel axis

v = current velocity perpendicular to the channel axis

θ = direction of the velocity vector relative to the channel axis

It was found that there was substantial scatter in the velocity data, especially near slack tides where the magnitude of the velocity vector was near that of the instrument resolution (commonly accepted as roughly 3 centimeters/second). This scatter was probably due to both the insensitivity of the instrument relative to such low velocities and to fluctuations caused by large-scale turbulent eddies. Data for the measured velocities appear in Appendix A.

The friction velocity for each data set was computed by using the Von Karman-Prandtl logarithmic expression given in Equation 7. A least-squares linear regression fit was made to the semilog plot of velocity versus the log of the height above the bed. An example profile is shown in Figure 8. The slope of this line is k_*/U, and the intercept is z_o. A Von Karman's constant of 0.4 was used in the analysis. Due to the scatter in the data, it was deemed inappropriate to attempt to look at trends beyond the linear. This rules out any effort to describe variations in the value of the constant due to density stratification (i.e., Richardson damping).

Friction velocity values were also obtained from the time series data in a similar manner. These values, obtained from only two data points each, were compared to that of the profiles (20 to 25 points each) to determine the error introduced by reducing the number of data points. In general, it was found that the two-point estimates were reasonably reliable. Data for all calculated friction velocities appear in Appendix B. Based upon these friction velocities, values for the bed shear stress were computed using Equation 8. These values will be used in conjunction with the suspended sediment concentration data and Equation 1 to determine field values of the critical shear stress and erosion rate coefficient.

Concentration Data

Five optical backscatterance sensors were used to measure the suspended sediment concentration. This sensor determines the amount of backward scattering of infrared light caused by a water sample (Downing, et al., 1981), and relates it to the particulate concentration via instrument calibration. The sensors described herein were calibrated in the laboratory both before and after the experiment using samples of sediment taken from the sediment/water interface of the experiment site. Figure 9 shows an example calibration for these sensors.

Each recorded data point was an average of ten measured points taken over 3 seconds. This approach was adopted in an attempt to reduce any scatter that might have been caused by small-scale turbulence. Both profile and time series data were collected. These data are preserved in Appendix C.

From a comparison of the shear stress time series with that of the suspended sediment concentration, it was noted that reasonable correlations were only observed for the ebb tide data. The flood tide concentration events, which included much larger suspended sediment concentration levels than did the ebb, did not correspond at all with the higher shear stresses as should be expected. Based upon past studies of the siltation mechanism at Mare Island, the following explanation is offered. Mare Island Strait is a small, deep channel that is appended to Carquinez Strait very near to its effluence into San Pablo Bay (see Figure 5).

Carquinez Strait is a deep channel with extremely fast currents (in some areas it has scoured to a depth of 70 feet). San Pablo Bay is a shallow muddy embayment of substantial fetch. The waves generated by the typical onshore winds suspend mud in the flats near the mouth of the Strait. The combination of the intense mixing in Carquinez Strait and the wave-generated mud suspension in San Pablo Bay creates an ample source of suspended sediment that is washed into Mare Island Strait during the flood tide (Krone, 1987). Using this information, it is argued that the flood tide concentration events were not resuspension events caused by local surface erosion, but rather an advection of suspended sediment that was resuspended outside the zone of the assumed uniform flow. With this argument as justification, the flood tide data were removed from consideration in the analysis that is described below.

Because suspended sediment concentrations in the lower regions of the bottom boundary layer were smaller than expected, the lower two optical backscatterance sensors were out of their operating range for much of the time. They only operated during resuspension events. Yet, it is necessary to have these values to obtain the total suspended load for a given time. Due to this problem it was necessary to attempt to extrapolate the concentration curves to cover the lower region of the bottom boundary layer for times of low suspended sediment concentrations. This extrapolation was based on Equation 6. A least-squares linear regression fit was made to the log-log plot of concentration versus dimensionless depth, $[(h-z)/z][a/(h-a)]$. The slope of this line is equal to the exponent, W_s/kU_*. Based on this exponent, the concentrations were found for the two stations in which data were missing.

The rate of surface erosion has dimensions of mass eroded per unit time. This can also be expressed as the time derivative of the total suspended sediment load. Thus, by substituting this expression into Equation 1 and rearranging:

$$\tau_b = \left(\frac{\tau_c}{M}\right)\left[\frac{d\ (TSL)}{dt}\right] + \tau_c \qquad (10)$$

where $\frac{d(TSL)}{dt}$ = the time derivative of the total suspended load.

A least-squares linear regression fit was made to the plot of bed shear stress versus the time derivative of the total suspended load. The slope of the line is τ_c/M, and the y-intercept is the critical shear stress (Figure 10). Based on this information, the critical shear stress (τ_c) of the surface layer of sediment in Mare Island Strait is 1.44 dynes/square centimeter. The erosion rate coefficient (M) is estimated as 3.5×10^{-2} milligrams/square centimeter-minute.

As a check, the critical shear stress (τ_c) was estimated in a second manner, utilizing data for a concentration increase for each of the five measured erosion events. The bed shear stress value corresponding to the inception of an increase in suspended sediment concentration was noted. Because both the concentration sensor position and the finite sampling interval allow a time lag, it was assumed that the increase in concentration actually began a short time before the sensors detected it (sometime between the detection reading and the previous

one). Therefore, the bed shear stress at both the point of detection of the increase in concentration and at the previous point were considered. The critical shear stress, as defined by Equation 1, is a constant for a given sediment type and depth into the seabed. Therefore, it is reasonable to assume that the same value of bed shear stress that is critical for this given situation must be present in all five of the measured erosion events. Allowing for some measurement uncertainty, the only range of bed shear stresses that is present in all five measured erosion events is 1.0 to 1.3 dynes/square centimeter (Figure 11). This is in reasonable agreement with the more precise value of 1.44, found with the previous method.

The other key parameter in Equation 10, the erosion rate coefficient (M), is probably slightly underestimated. The flux of sediment into the upper water column was not taken into consideration in the calculation of the total suspended sediment load. This flux would occur as a gradual process through the later stages of the resuspension event. This suggests that the time derivative of the total suspended load, especially in the higher portions of the curve, is underestimated. An attempt has been made to estimate the magnitude of this error by using the Rouse equation to extrapolate the sediment concentration data into this portion of the water column. These efforts suggest that the error is up to 15 percent, thus offering a possible range of values of M from 3.5×10^{-2} to 4.0×10^{-2} milligrams/square centimeter-minute.

Apparent Settling Velocity

An apparent settling velocity was estimated using Equation 6. A least-squares linear regression fit was made to the log-log plot of concentration versus dimensionless depth, $[((h-z)/z)(a/(h-a))]$. The slope of this line is equal to the exponent, W_s/kU_*. Both k and U_* are known for each set of measurements; therefore, the settling velocity, W_s can be obtained. This procedure was performed for both the profile data and the time series data. Fair agreement was found between them. A graph of these values can be found in Appendix D.

The apparent settling velocity data (profile data only) were compared to concentration, velocity, and friction velocity data in an attempt to correlate the apparent settling velocity to more easily measured parameters. No correlation was found with either the fluid velocity or the friction velocity. A weak correlation was found between the apparent settling velocity and the suspended sediment concentration. This correlation is shown in Figure 12. A number of settling velocity experiments have been conducted in quiescent waters (Krone, 1962; Owen, 1970; Kranck, 1986) that have considered similar correlations. Results show that the sediment concentration is a strong factor in determining the settling velocity, but that the relationship is not linear. The exponents cited have ranged from 1.0 to 2.5 for saline water (van Leussen, 1988). The field data presented herein are not of sufficiently high resolution to determine whether or not a better fit would be obtained by using an exponent other than one.

In standard settling velocity experiments in quiescent waters the dominant cause of flocculation is collision of particles due to the different settling rates of different sized aggregates. It has been

suggested (Krone, 1972) that this cause is actually of secondary importance when compared to the collisions caused by internal shearing of the fluid flow. Therefore, the effects of the friction velocity were included in the apparent settling velocity versus sediment concentration comparison. A much stronger correlation was found than was seen when comparing the apparent settling velocity with concentration alone (Figure 13). This result supports Krone's inference, and casts a shadow of doubt over all of the efforts to extrapolate a field settling velocity from experiments conducted under quiescent conditions.

Some of the time series data sets had five points available from which to obtain the apparent settling velocity. Most had only three points. An apparent settling velocity was calculated for the five-point data sets using both five points and the three points that were available in the rest of the data sets. It was noted that the apparent settling velocity values were generally higher when five points were used in the estimation process. This suggests that the settling velocity may be larger in the lower portions of the water column. This inference is supported by data presented in Sternberg et al. (1986) that indicate that aggregate particle size is typically larger in the lower portions of the water column. If the settling velocity varies significantly with depth, the equations describing deposition and transportation may require revision.

SUMMARY

A field experiment was conducted to gather data, which were then used to evaluate methods for predicting cohesive sediment transport.

Erosion

Equation 1 is typically used to describe surface erosion. In this equation there are two parameters that are not easily defined: the erosion rate coefficient (M), and the critical shear stress of erosion initiation (τ_c). Both have been predicted, using various methods, in the laboratory. A field experiment was performed to evaluate both the applicability of Equation 1 and the usefulness of the laboratory predictions of these parameters. In support of Equation 1, we find that a linear equation best relates the erosion rate to the bed shear stress. A comparison was made of the measured values of both the critical shear stress and the erosion rate coefficient to those values predicted in the laboratory. We found that flume experiments using naturally deposited sediment beds do a reasonable job in predicting these parameters, but that experiments using remolded sediments do not approximate the conditions encountered in the field.

Deposition

Equation 2 is typically used to describe the deposition of cohesive sediments. The parameter described as the critical shear stress of deposition is rather ill-defined. It refers to a bed shear stress at which all of the suspended sediment load will eventually fall out of suspension. All of the values presented in Table 2 were obtained in

flumes that maintained a constant shear stress. Due to the nature of field experiments (i.e., no control over the shear stresses) it is not possible to measure this parameter directly.

Transportation

Equation 5 is typically used to describe the transportation of suspended sediments. Modeling difficulties are encountered when one attempts to define the vertical distribution of the suspended sediment concentration using Equation 6. Two parameters in this equation pose difficulties: the settling velocity and the reference concentration.

The settling velocity is typically assumed to be a constant for modeling purposes. This is not in keeping with the fluctuations seen in the apparent settling velocity data that were calculated from the field data. The apparent settling velocity changed more than one order of magnitude over the duration of a tidal cycle. The assumption that the settling velocity is a constant is certainly an oversimplification. We have found no viable means of predicting the settling velocity in the laboratory. The standard means of estimating the "constant settling velocity" in the laboratory (still-water settling) does not take into account internal shearing, which is the dominant process in determining the field settling velocities of flocculated materials.

Although the issue of reference concentration was not directly addressed in this experiment, the following observation can be made based on the data collected. It appears that there is some background level of suspended sediment concentration that was returned to after each resuspension event. Since most resuspension events do not involve the entire water column (at least in artificially-deepened estuaries), there must be some level, close to the surface, that maintains a relatively constant level of suspended sediment concentration. It is also likely that the concentration at this level would be reasonably uniform over a wide expanse of the estuary. This is just speculation, but it suggests that there may be a possibility of obtaining the reference concentration with a single set of measurements specifying the background concentration.

CONCLUSIONS

1. A linear equation best relates the erosion rate to the bed shear stress:

$$E = M\left(\frac{\tau_b - \tau_c}{\tau_c}\right)$$

2. Flume experiments using naturally deposited sediment beds do a reasonable job in predicting the values of both the critical shear stress and the erosion rate coefficient. Laboratory test using remolded sediments do a poor job of predicting these values.

3. The settling velocity is normally assumed to be a constant, but this research suggests that the settling velocity can vary by over an order of magnitude during a single tide cycle.

REFERENCES

Adams, C.E., and Weatherly, G.L. (1981). "Suspended sediment transport and benthic boundary layer dynamics," Marine Geology, vol 42, 1981, pp 1-18.

Ariathurai, R., and Arulanandan, K. (1978). "Erosion rates of cohesive soils," Journal of the Hydraulics Division, vol 104, no. HY2, 1978, pg 279.

Downing, J.P., Sternberg, R.W., and Lister, C.R.B. (1981). "New instrumentation for the investigation of sediment suspension processes in the shallow marine environment," Marine Geology, vol 42, 1981, pp 19-34.

Kranck, K. (1986). "Settling behavior of cohesive sediment," Lecture Notes on Coastal and Estuarine Studies, vol 14, editor: A.J. Mehta. New York, NY, Springer-Verlag Publishing Co., 1986, pp 151-169.

Krone, R.B. (1962). Flume studies of the transport of sediment in estuarial shoaling processes, University of California at Berkeley, Hydraulic Engineering Laboratory and Sanitary Engineering Research Laboratory, Final Report to San Francisco District, United States Army Corps of Engineers (USACOE). Berkeley, CA, 1962.

Krone, R.B. (1972). "A field study of flocculation as a factor in estuarial shoaling processes," Committee on Tidal Hydraulics, USACOE, Technical Bulletin No. 19, 1972.

Krone, R.B. (1987). Personal communication, University of California, Davis, CA, 23 Mar 1987.

Malloy, R.J. (1980). U.S. Navy harbor maintenance dredging atlas, Naval Civil Engineering Laboratory, Technical Note N-1597. Port Hueneme, CA, 1980.

Mehta, A.J. (1986). "Characterization of cohesive sediment properties and transport processes in estuaries," Lecture Notes on Coastal and Estuarine Studies, vol 14, Estuarine Cohesive Sediment Dynamics. New York, NY, Springer-Verlag, 1986, pg 290.

Mehta, A.J., Parchure, T.M., Dixit, J.G., and Ariathurai, R. (1982). "Resuspension potential of deposited cohesive sediment beds," Estuarine Comparisons. San Diego, CA, Academic Press, Inc., 1982, pp 591-609.

Ockenden, M.C., and Delo, E.A. (1988). Consolidation and erosion of estuarine mud and sand mixtures, Hydraulics Research, Ltd., Report No. SR 149. Wallingford, England, 1988.

Owen, M.W. (1970). A detailed study of the settling velocities of an estuary mud, Hydraulic Research, Ltd., HR Report No. 78. Wallingford, England, 1970.

Parchure, T.M., and Mehta, A.J. (1985). "Erosion of soft cohesive sediment deposits," Journal of Hydraulic Engineering, vol 111, no. 10, 1985, pp 1308-1326.

Partheniades, E. (1962). A study of erosion and deposition of cohesive soils in salt water," Ph.D. thesis, University of California at Berkeley, CA, 1962.

Rouse, H. (1938). "Experiments on the mechanics of sediment suspensions," in Proceedings of the Fifth International Congress for Applied Mechanics, Cambridge, MA, 1938.

Shi, N.C., Larsen, L.H., and Downing, J.P. (1985). "Predicting suspended sediment concentration on continental shelves," Marine Geology, vol 62, 1985, pp 255-276.

Sternberg, R.W., Cacchione, D.A., Drake, D.E., and Krank, K. (1986). "Suspended sediment transport in an estuarine tidal channel within San Francisco Bay, California," Marine Geology, vol 71, 1986, pp 237-257.

van Leussen, W. (1988). "Aggregation of particles, settling velocity of mud flocs: A review," Physical Processes in Estuaries, editors: J. Dronkers and W. van Leussen, New York, NY, Springer-Verlag Publishing Co., 1988.

Vanoni, V.A., and Nomicos, G.N. (1959). "Resistance properties of sediment laden streams," in Proceedings of the American Society of Civil Engineers, vol 85, no. HY5, 1959.

Table 1. Soil Shear Strength Zones as Measured in the Laboratory (Parchure and Mehta, 1985)

Shear Strength Zone	Range ($dynes/cm^2$)
τ_{so}	0.4 to 1.7
τ_{sc}	2.1 to 6.2
τ_{sm}	5.7 to 6.7

Table 2. Cited Values for Critical Shear Stress of Deposition

Reference	τ_{cd} ($dynes/c^2$
Krone (1962)	0.6
Ariathurai (1978)	0.2
Mehta (1986)	1.5
	1.0
	0.8

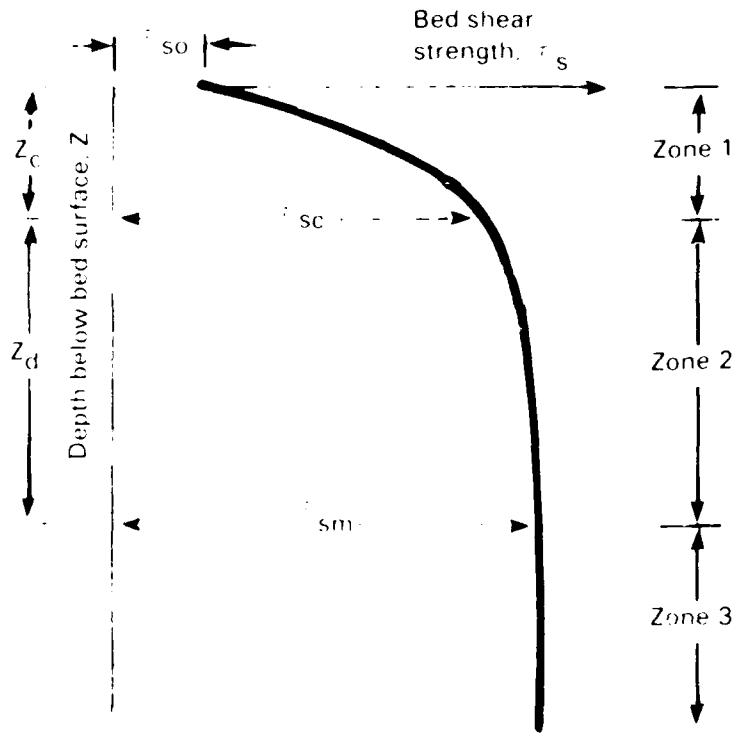

Figure 1. Schematic representation of three-zoned description of bed shear strength profile (from Parchure and Mehta, 1985).

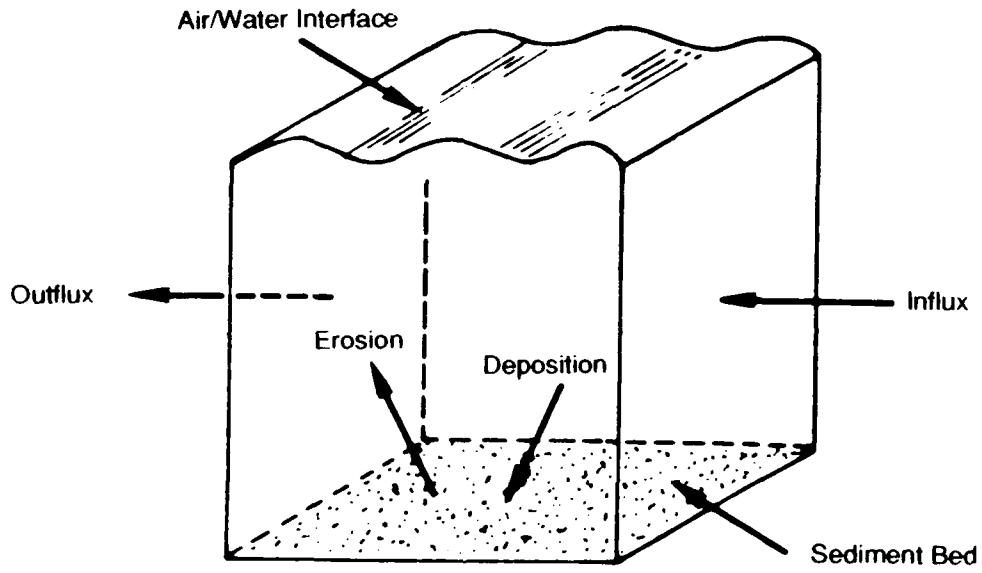

Figure 2. Flux of sediment through control volume.

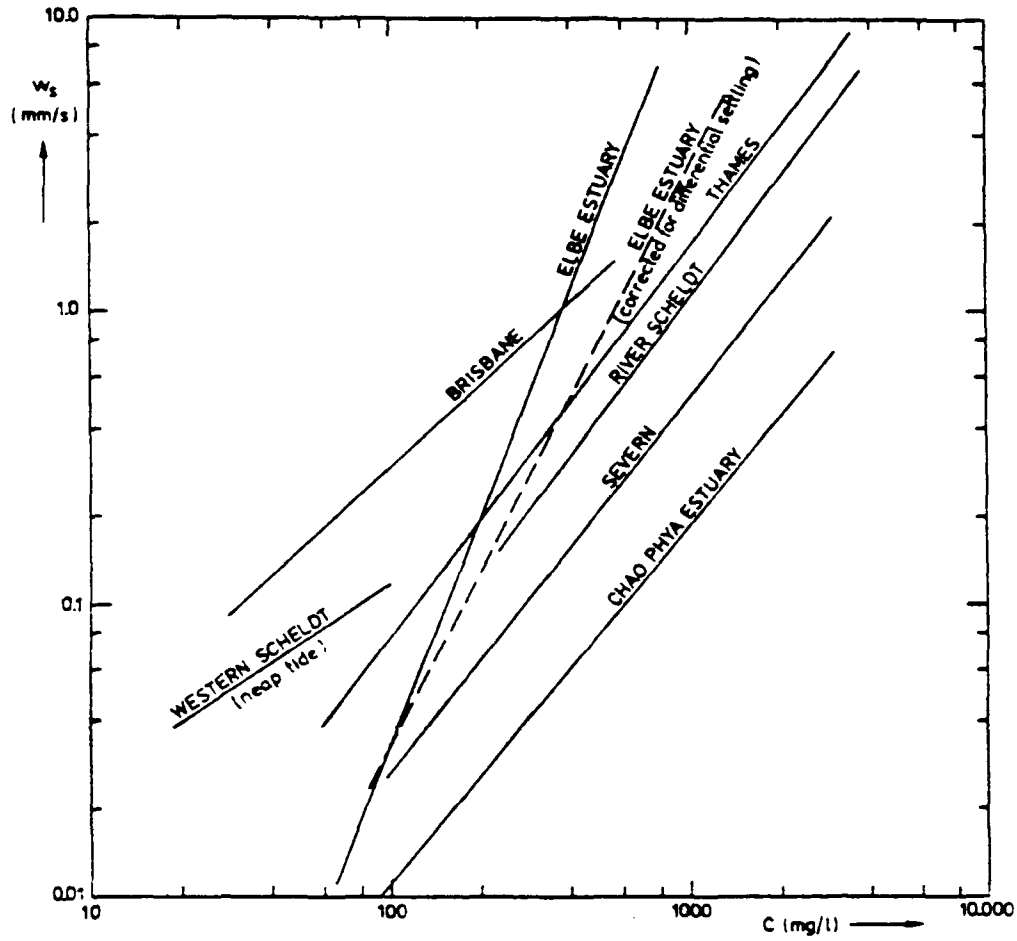

Figure 3. Median settling velocities of mud flocs as a function of concentration, measured by in-situ apparatus in saline water. Reprinted from Van Leuseen (1988).

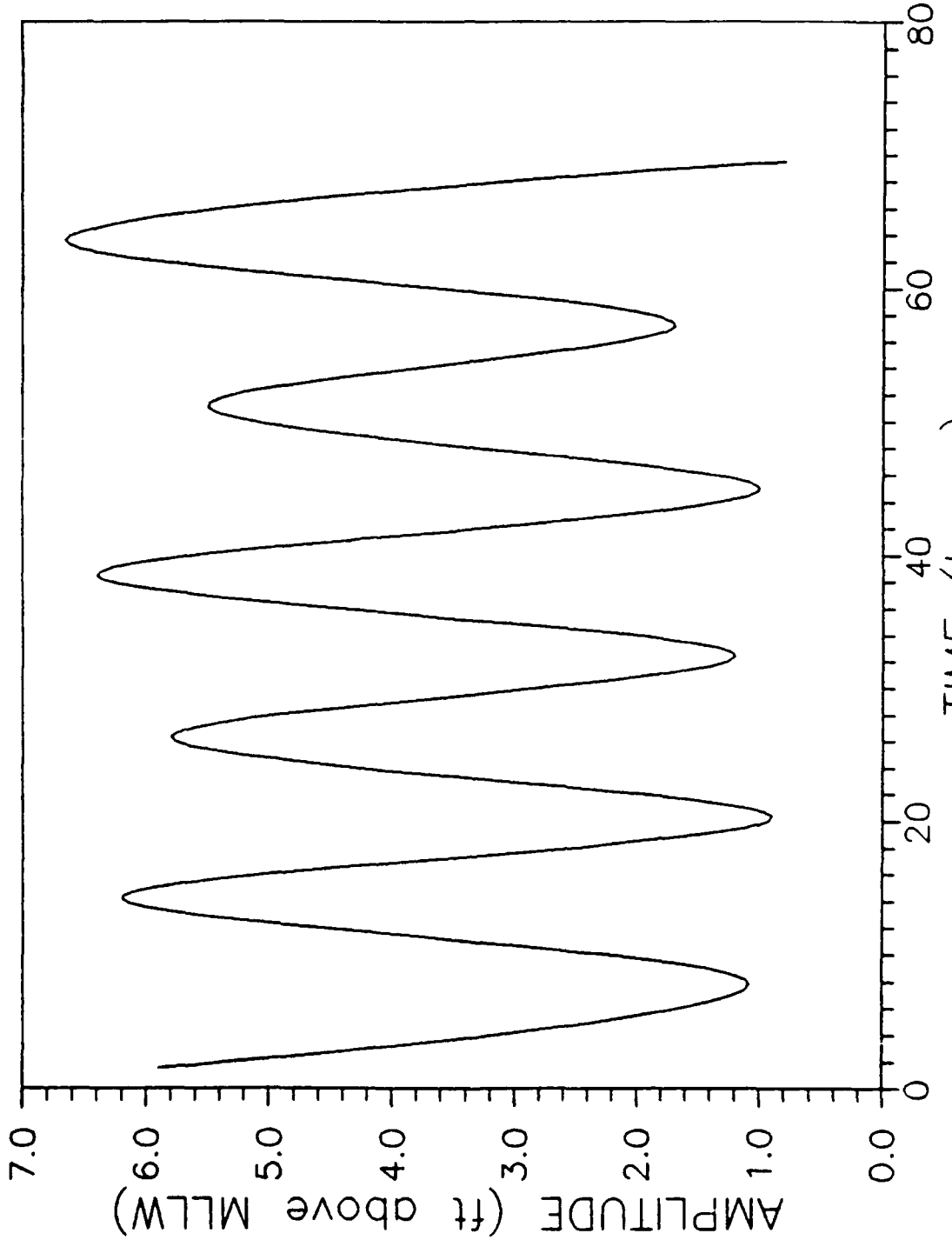

Figure 4. Tide data for the duration of the experiment.

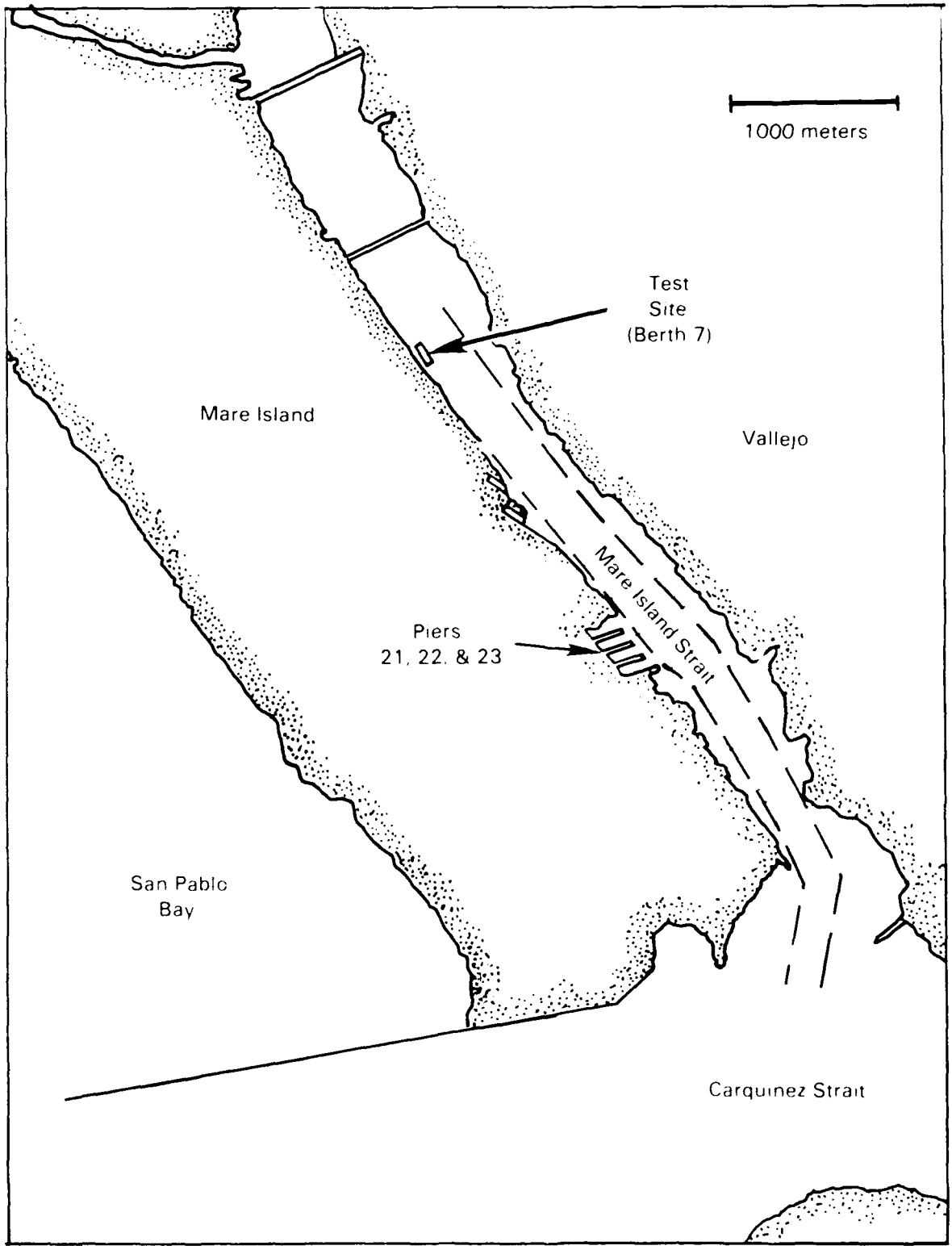

Figure 5. Location map of experiment site.

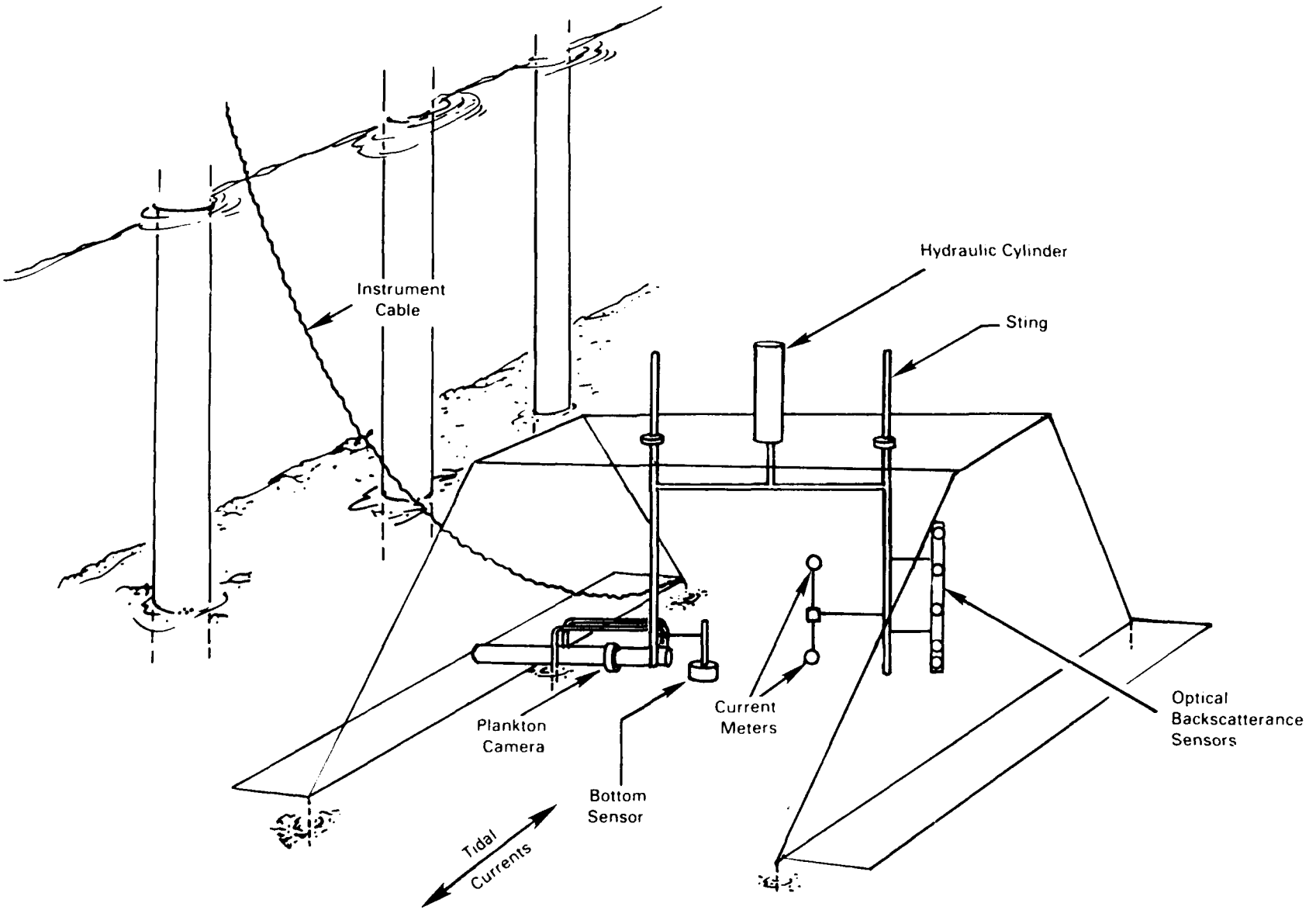

Figure 6. Seafloor landing framework and instrument sting.

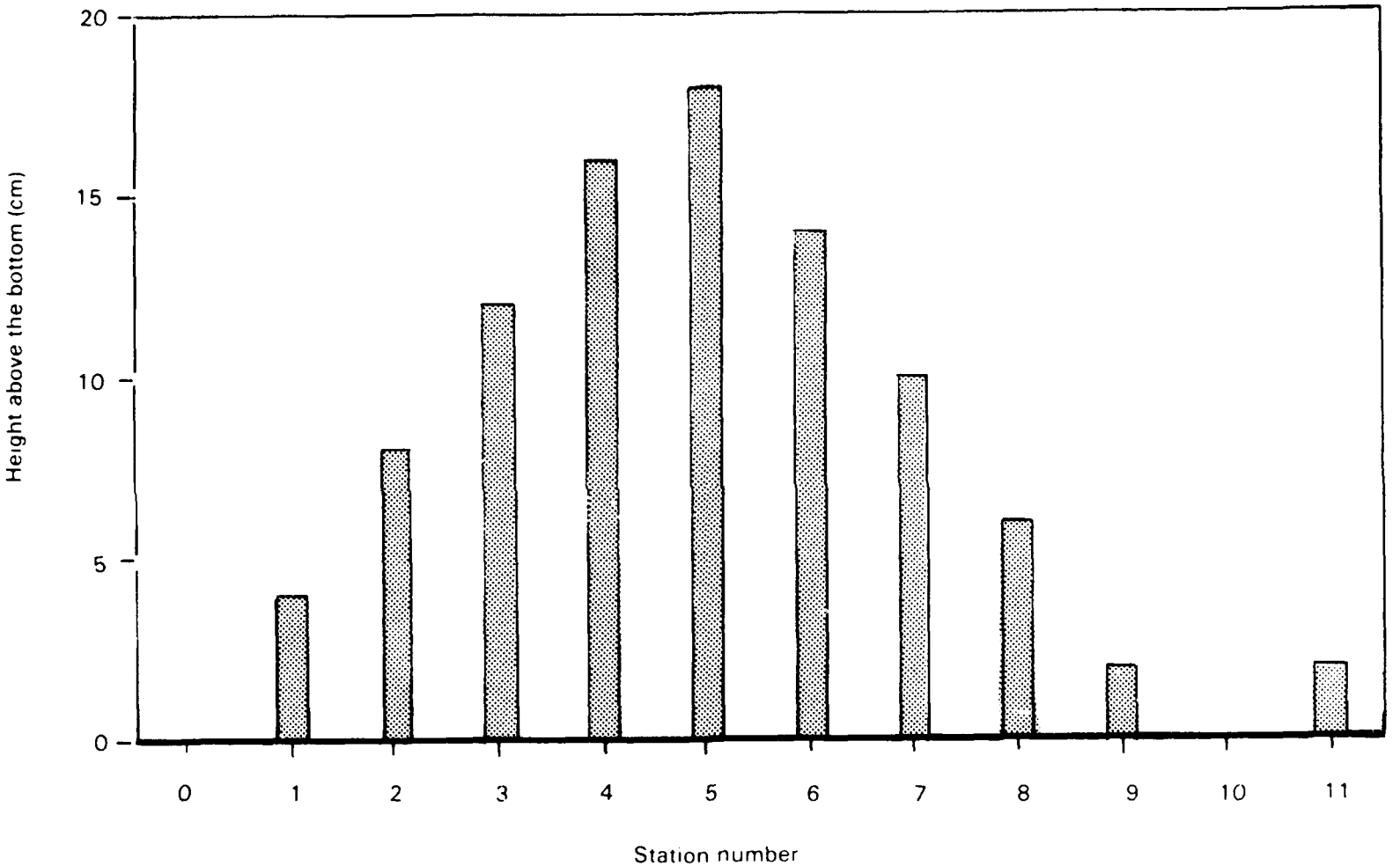

Figure 7. Stations at which measurements were recorded during a profile.

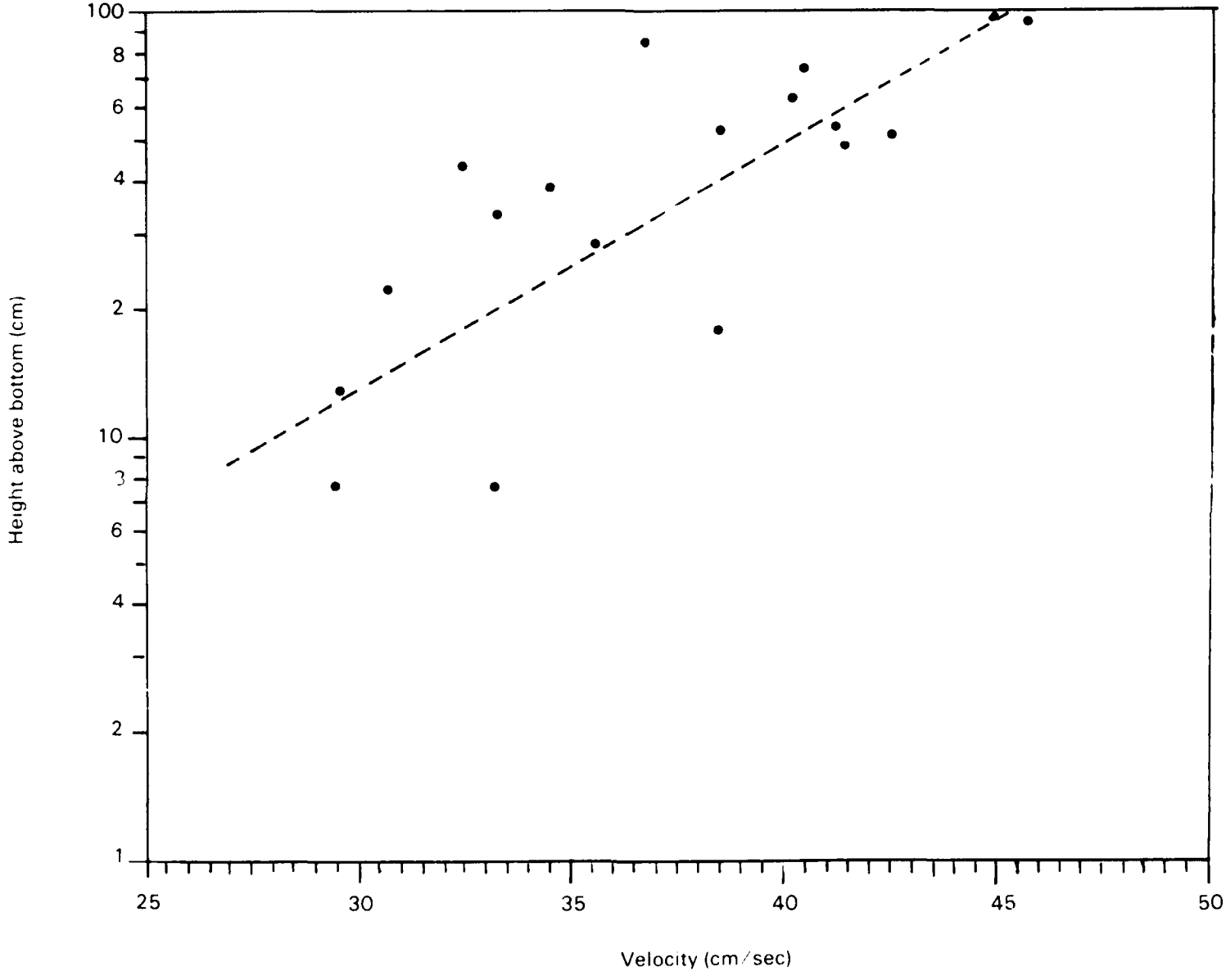

Figure 8. An example velocity profile. Both data points and linear regression fit are shown.

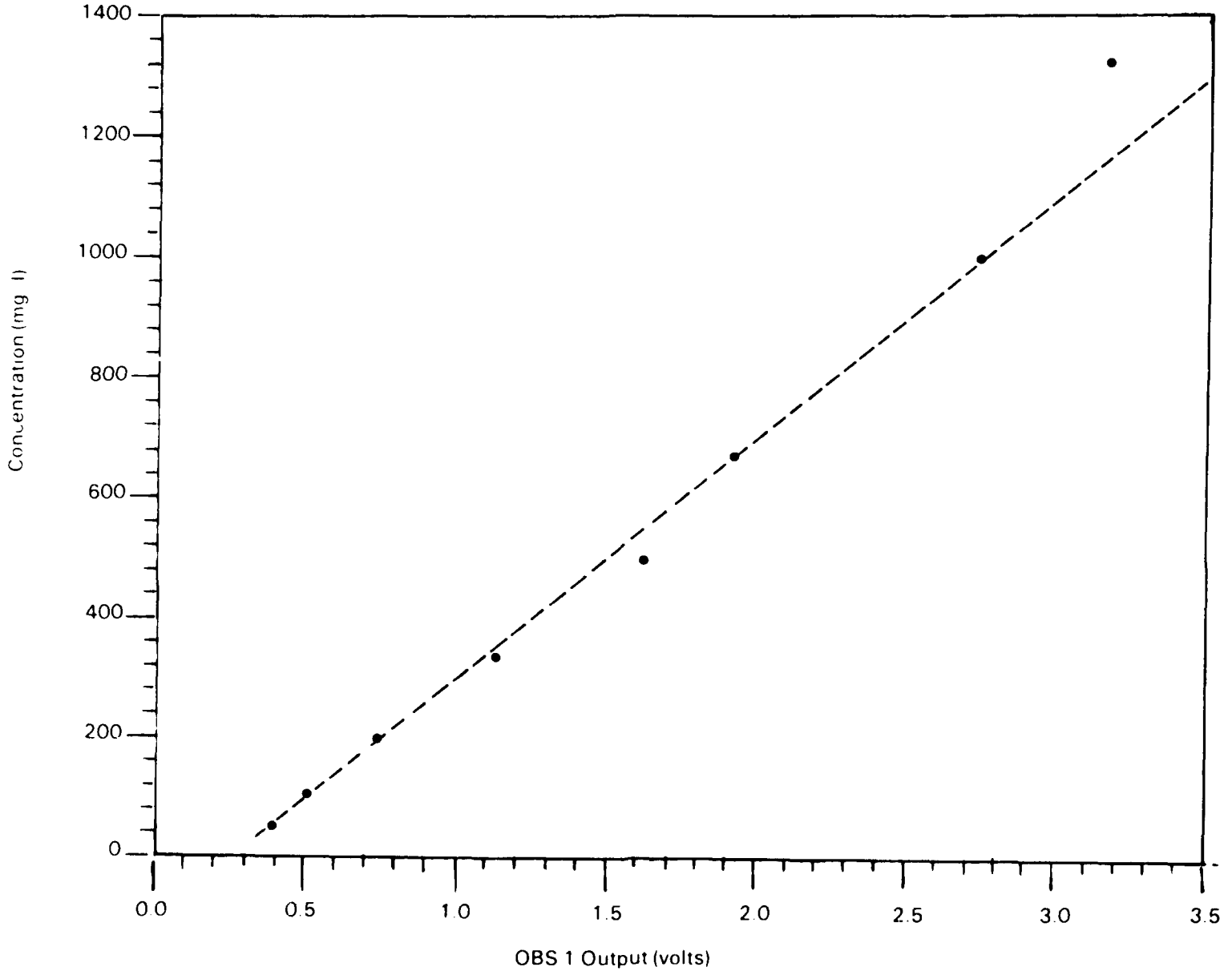

Figure 9. An example calibration of an optical backscatterance sensor.

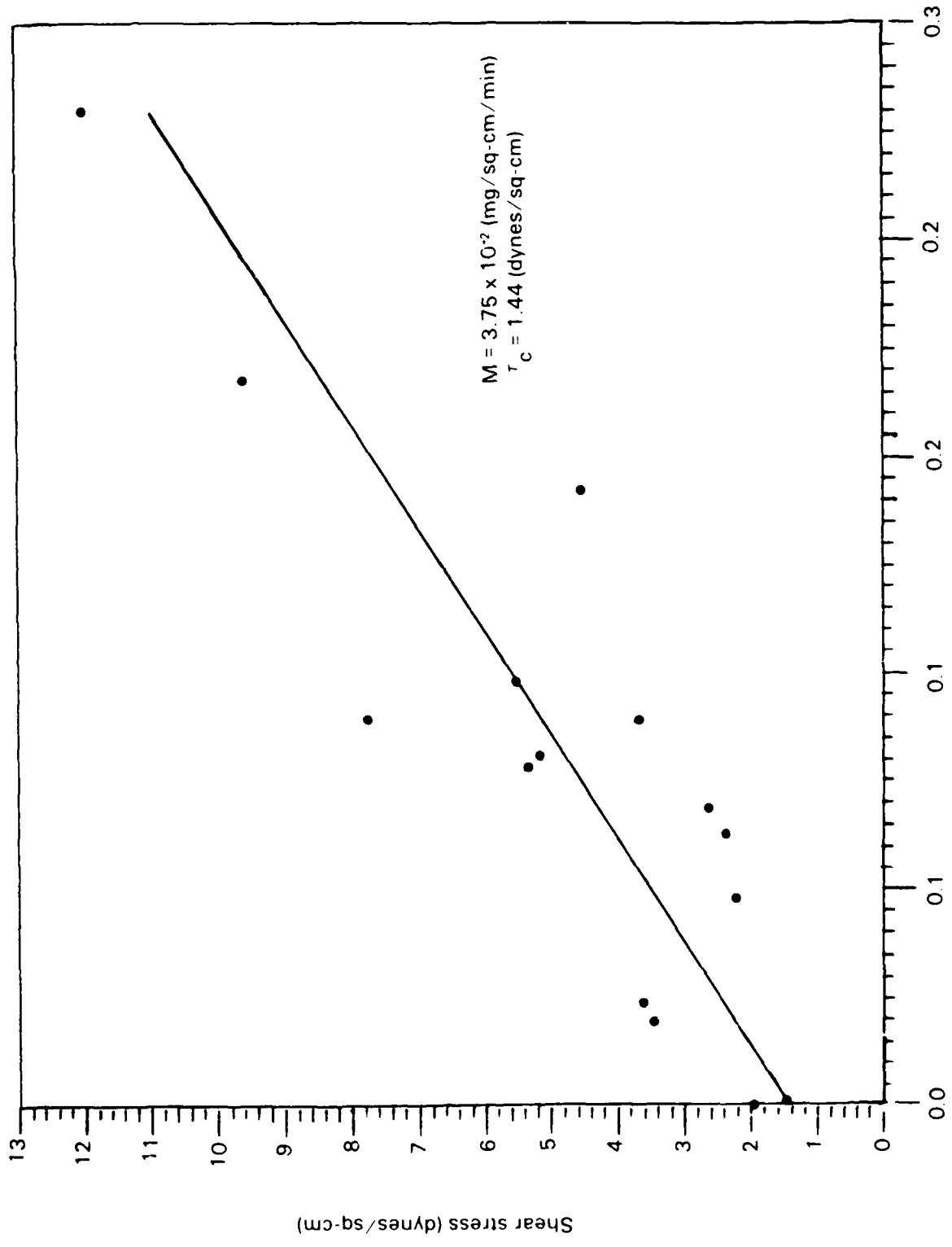

Figure 10. Bed shear stress versus the erosion rate.

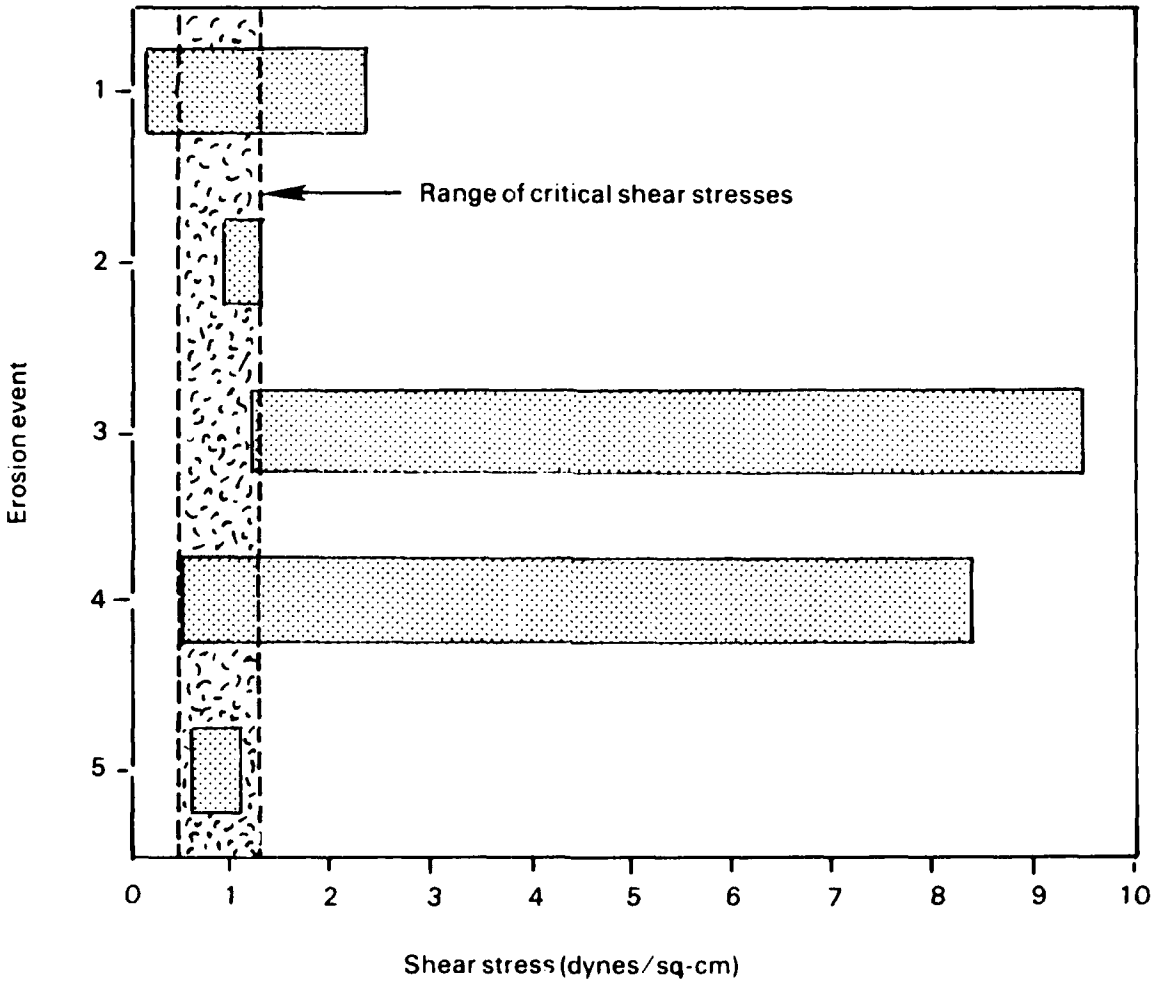

Figure 11. Shear stress values for observed erosion events.

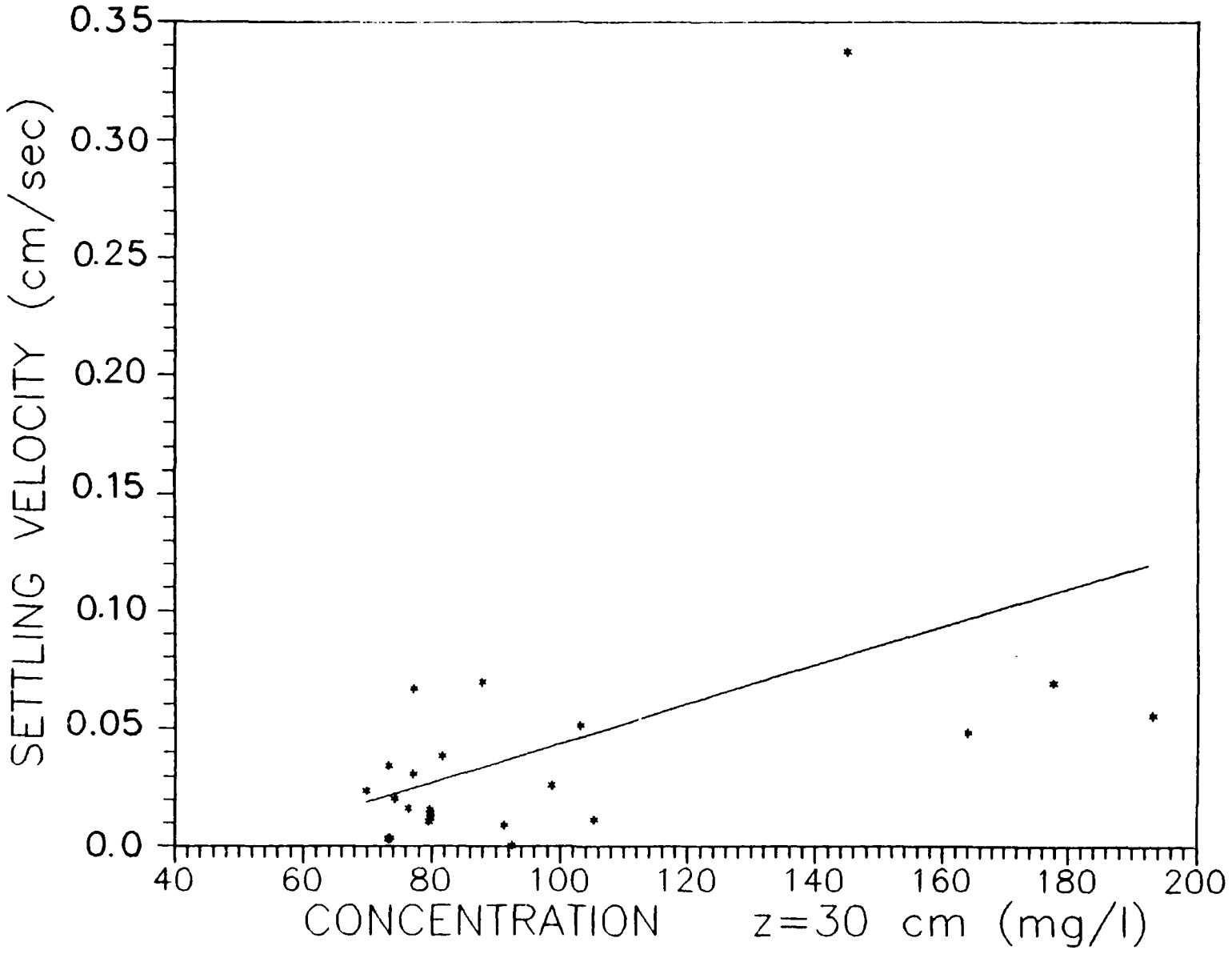

Figure 12. Apparent settling velocity versus a referenced sediment concentration.

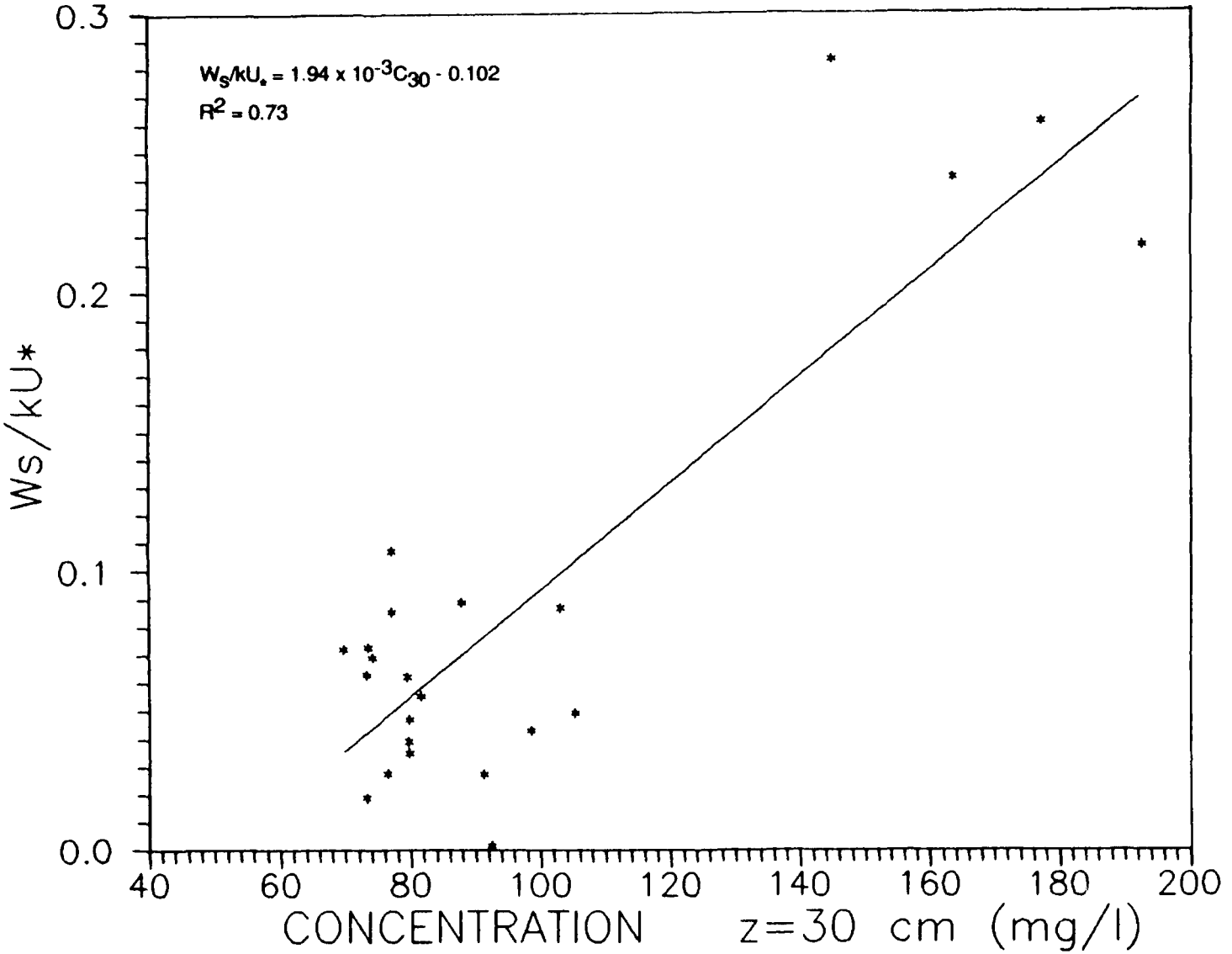

Figure 13. Rouse coefficient versus a referenced sediment concentration.

Appendix A

VELOCITY DATA

This appendix contains a graphical presentation of the time series velocity data. The data were presented as two horizontal velocity vectors at the indicated heights (16 and 62 cm) above the z-datum.

The time scale runs continuously from Figure A-1 through Figure A-5. The time 0000 hours on Figure A-1 is midnight at the beginning of the first day of the measurements. The time 5500 hours on Figure A-5 (for example) is 55 hours later (i.e., 7:00 a.m. the third day).

An averaging-type curve smoothing routine was used in which each velocity value was modified by the two adjacent values. The lines shown are smooth curves drawn through the given data points.

Vertical velocity distributions for the profile data can be obtained by using Equation 7 in the main text of this report with the friction velocity and roughness coefficient values given in Appendix B.

VELOCITY

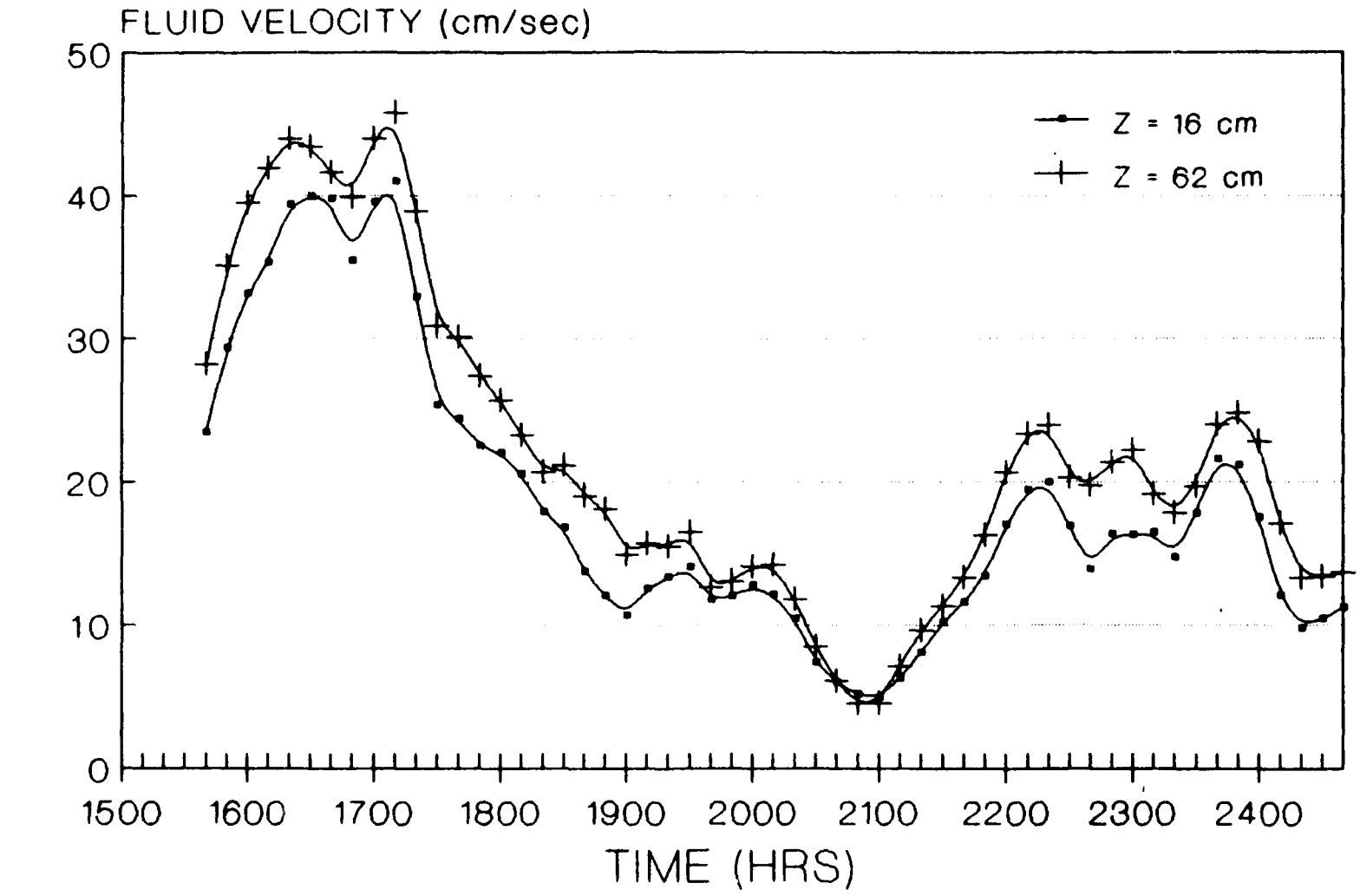

HALF HOUR AVERAGING

Figure A-1

VELOCITY

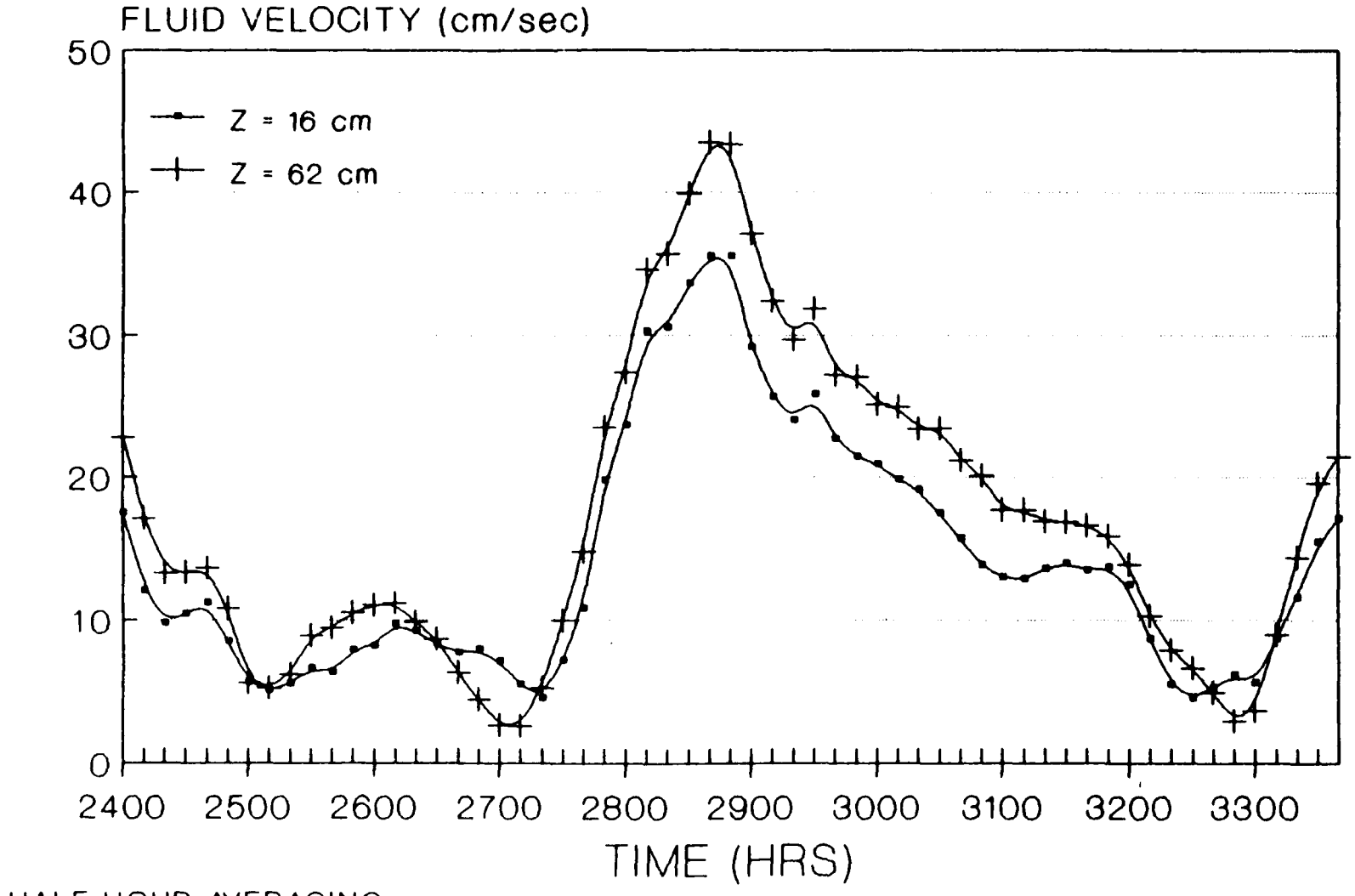

HALF HOUR AVERAGING

Figure A-2

VELOCITY

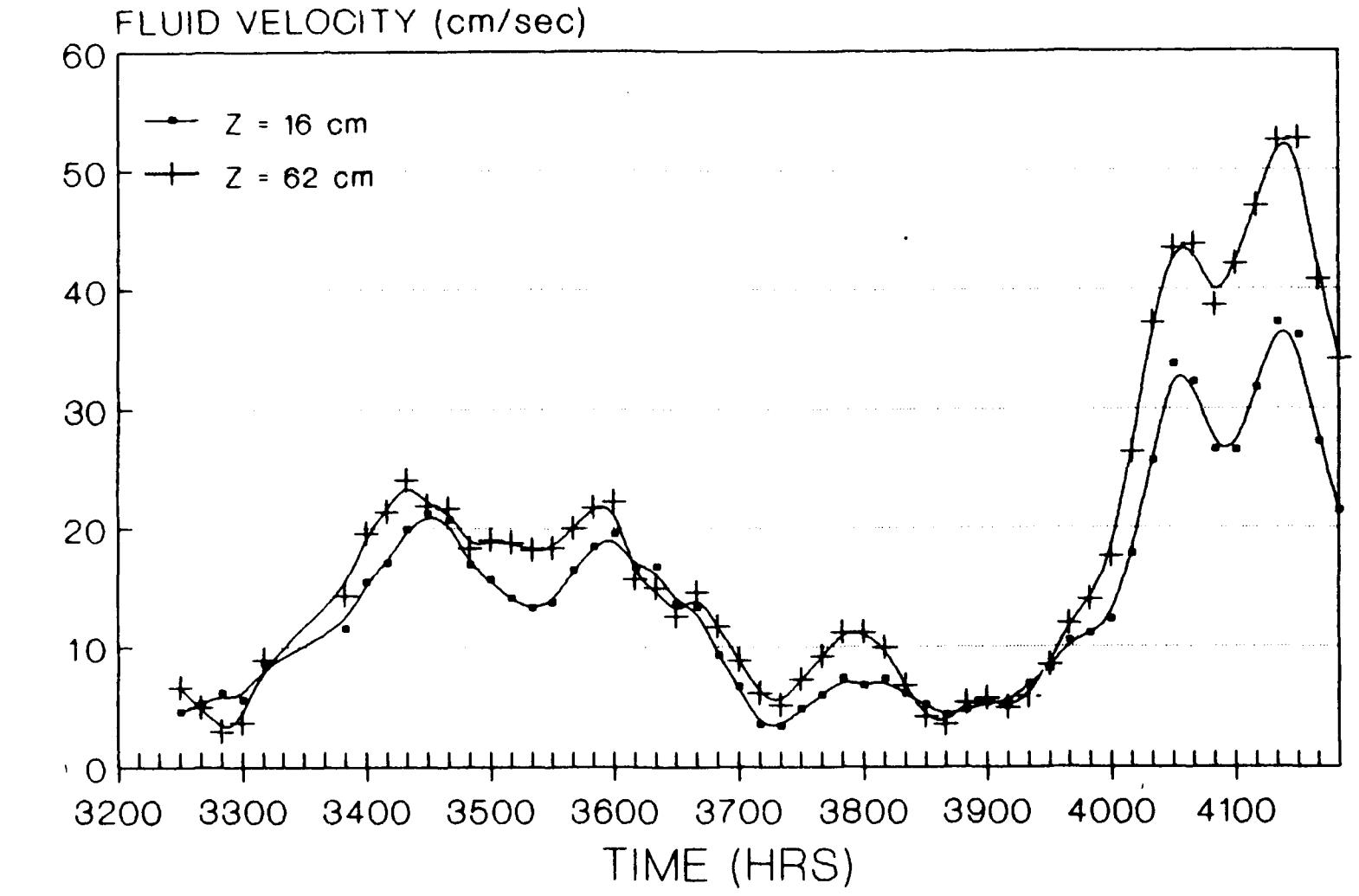

HALF HOUR AVERAGING

Figure A-3

VELOCITY

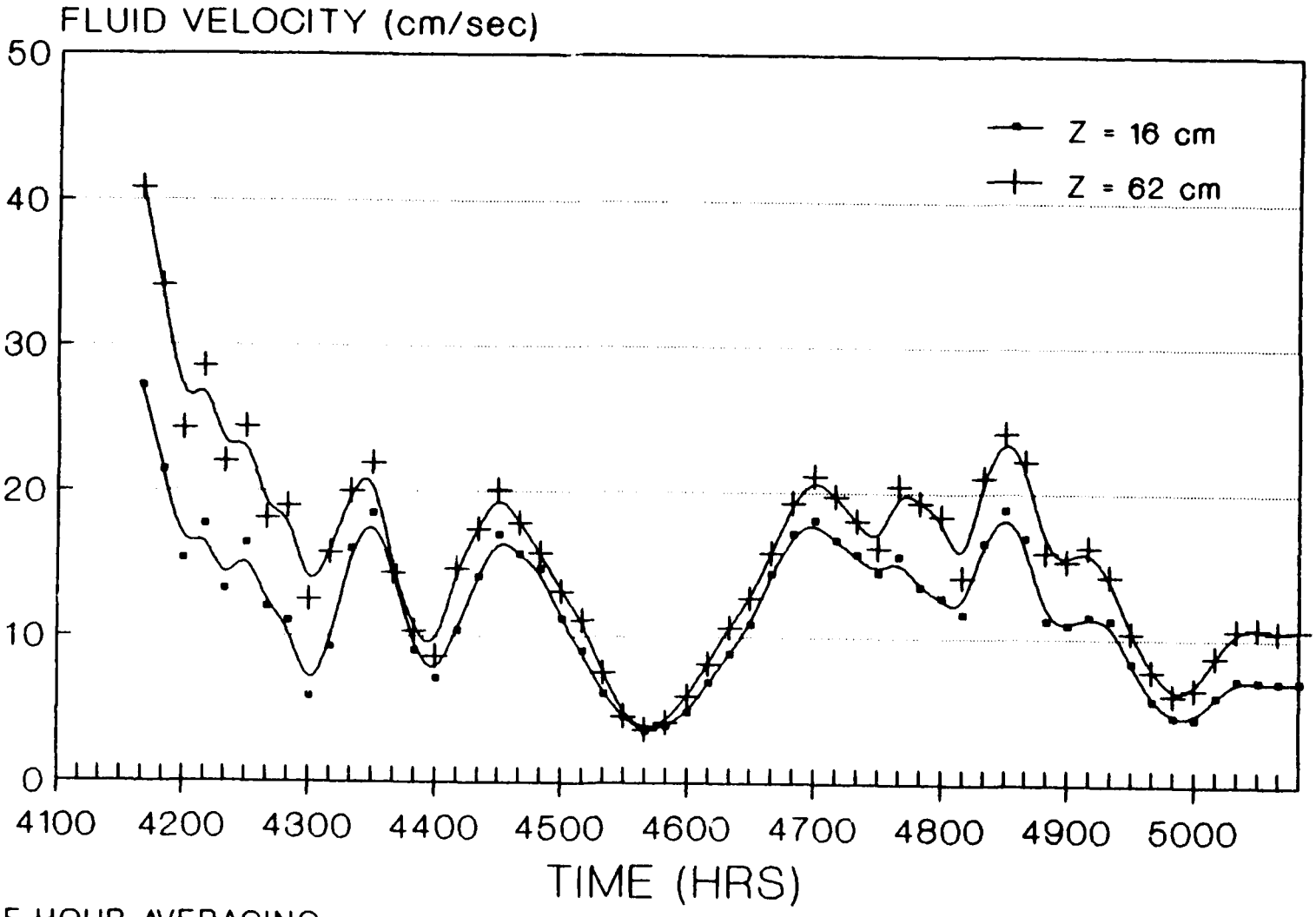

HALF HOUR AVERAGING

Figure A-4

VELOCITY

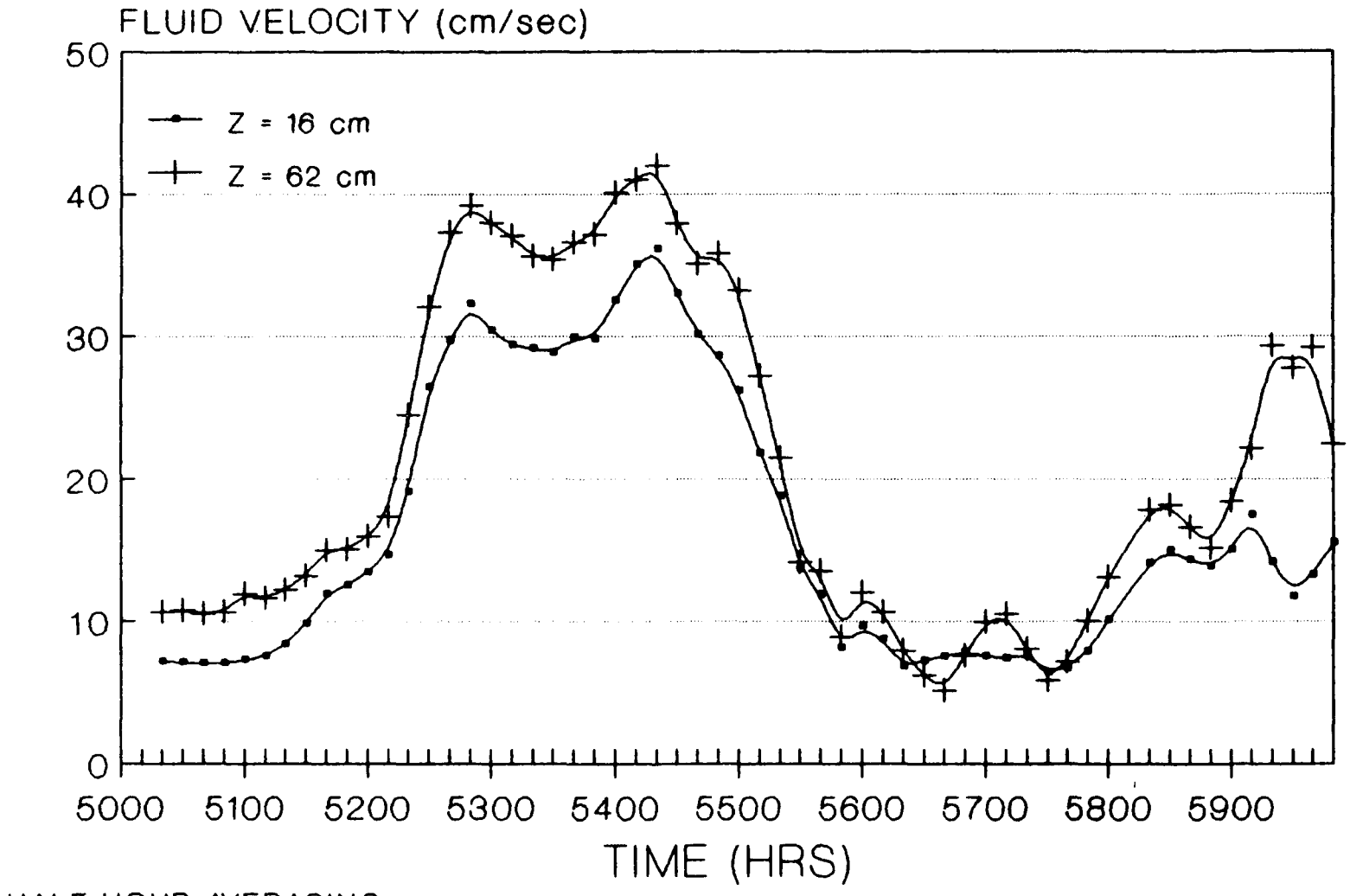

HALF HOUR AVERAGING

Figure A-5

Appendix B

FRICTION VELOCITY

This appendix contains a graphical presentation of the time series and profile friction velocity data (Figures B-1 through B-5) as well as a list of the profile data (Table B-1). The profile data list (Table B-1) contains the friction velocity and the roughness coefficient, both of which are based on the measured vertical distribution of the horizontal velocity vector.

The friction velocity time series data were computed, using Equation 7 in the main text of this report, from the velocity time series data shown in Appendix A. The time scale runs continuously from Figure A-1 through Figure A-5. The time 0000 hours on Figure A-1 is midnight at the beginning of the first day of the measurements. The time 5500 hours on Figure A-5 (for example) is 55 hours later (i.e., 7:00 a.m. for the third day). The line shown is a smooth curve drawn through the given data points.

Table B-1. PROFILE DATA

TABLE OF FRICTION VELOCITIES AND ROUGHNESS COEFFICIENTS

PROFILE (day-hr)	FRICTION VELOCITY (cm/sec)	ROUGHNESS COEFFICIENT (cm/sec)
266-1530	1.55	0.47
266-1600	1.95	0.49
266-1630	1.24	0
266-1700	1.75	0.002
266-1730	0.67	0
266-1800	1.52	0.11
267-0700	1.00	0.19
267-0730	0.64	0
267-0830	1.47	6.83
267-0900	0.12	0
267-0930	0.83	0.03
267-1000	1.37	0.31
267-1030	0.74	0
267-1100	0.91	0.05
267-1130	1.02	0.18
267-1200	0.82	0.02
267-1230	0.66	0.003
267-1300	0.50	0.03
267-1330	0.58	0.24
267-1400	0.83	0.40
267-1430	1.48	8.60
267-1500	0.64	0.46
267-1530	0.24	0
267-1600	1.23	0.50
267-1630	2.97	0.22
268-0730	0.43	0
268-0800	0.40	0
268-0900	1.30	4.66
268-0930	0.94	1.02
268-1000	0.88	0.02
268-1030	1.71	0.42
268-1100	1.10	0.03
268-1130	0.68	0.06
268-1200	0.29	0
268-1230	1.10	0.21
268-1300	0.30	0
268-1330	0.81	3.38

FRICTION VELOCITY

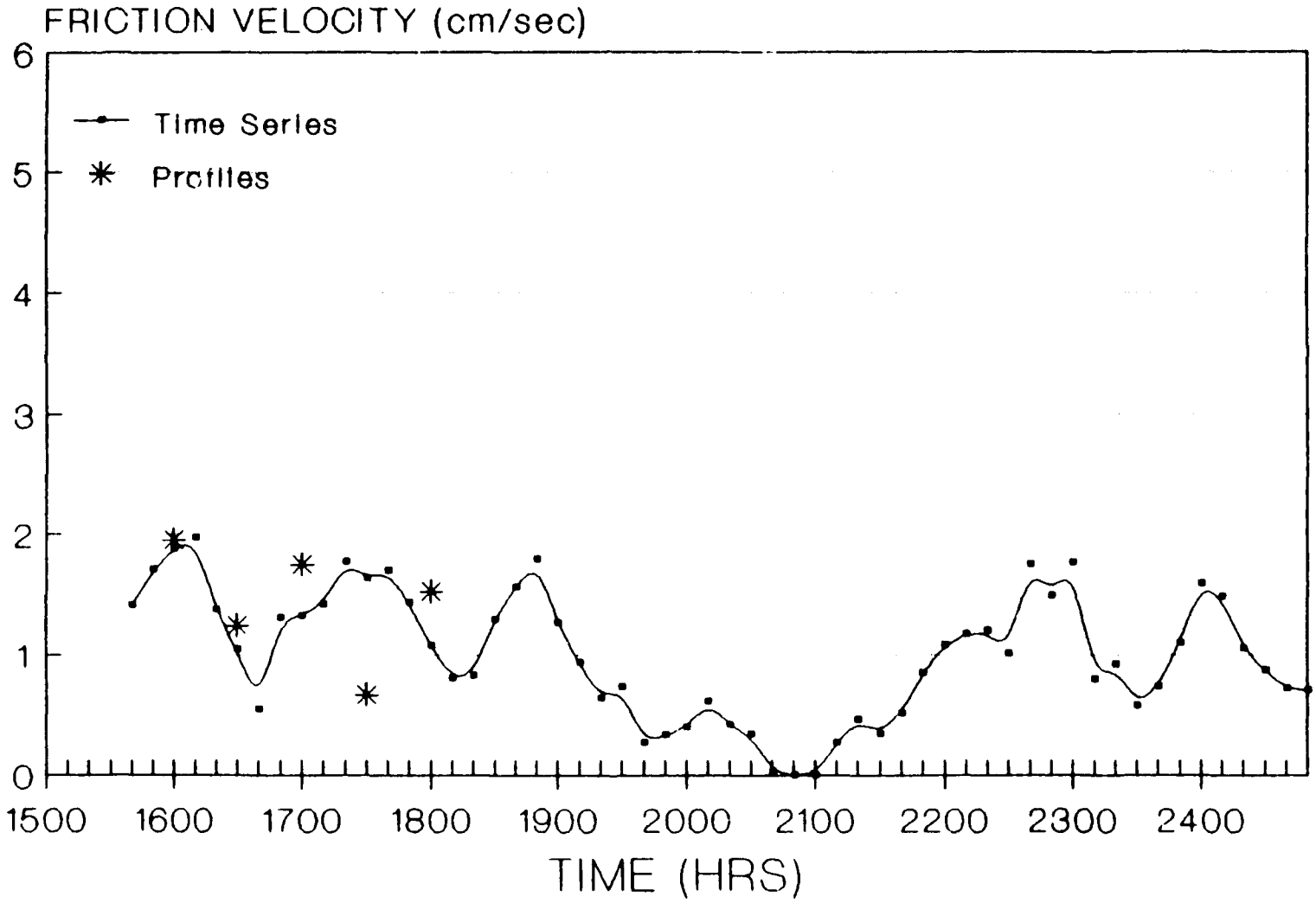

Figure B-1

FRICTION VELOCITY

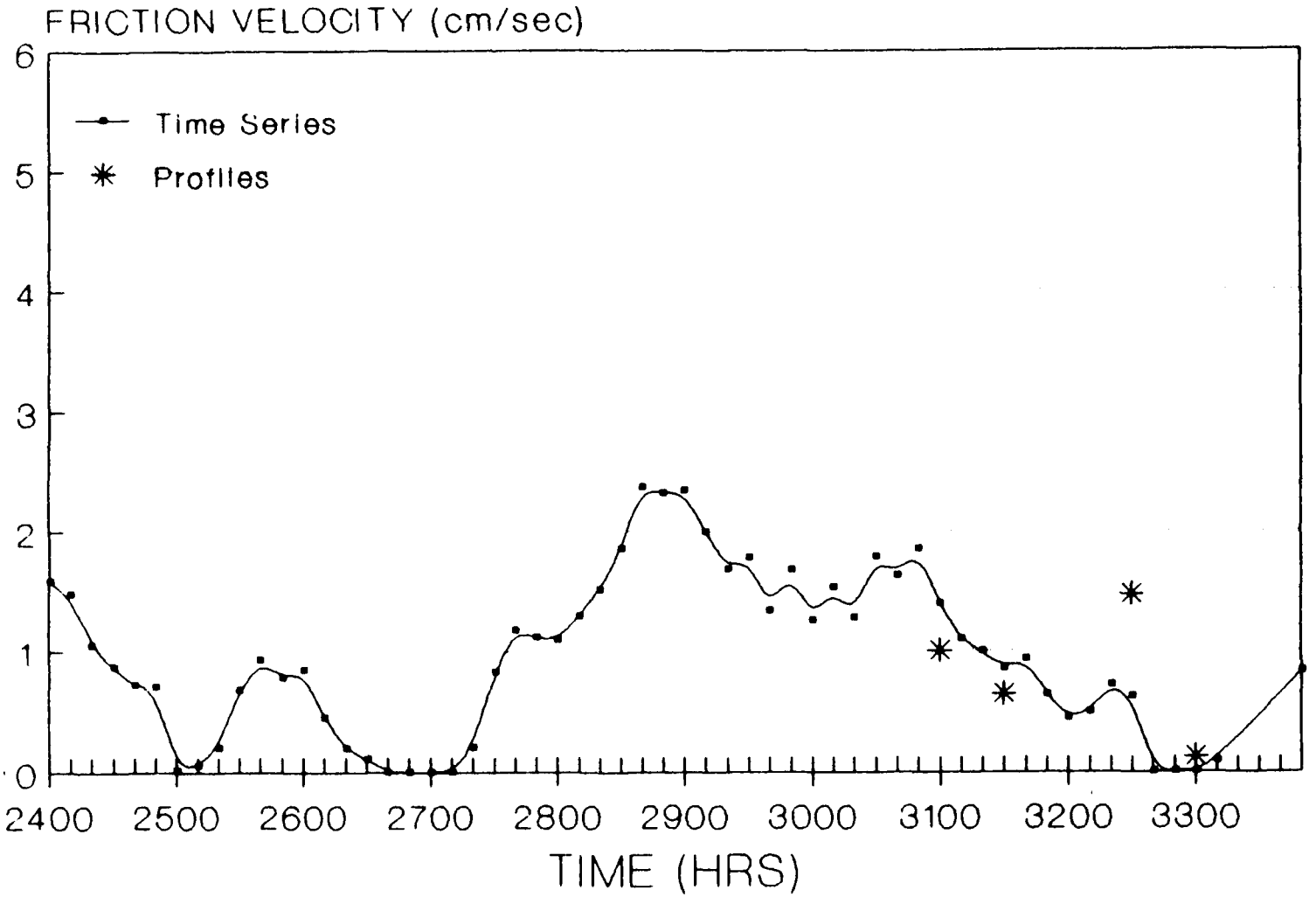

Figure B-2

FRICTION VELOCITY

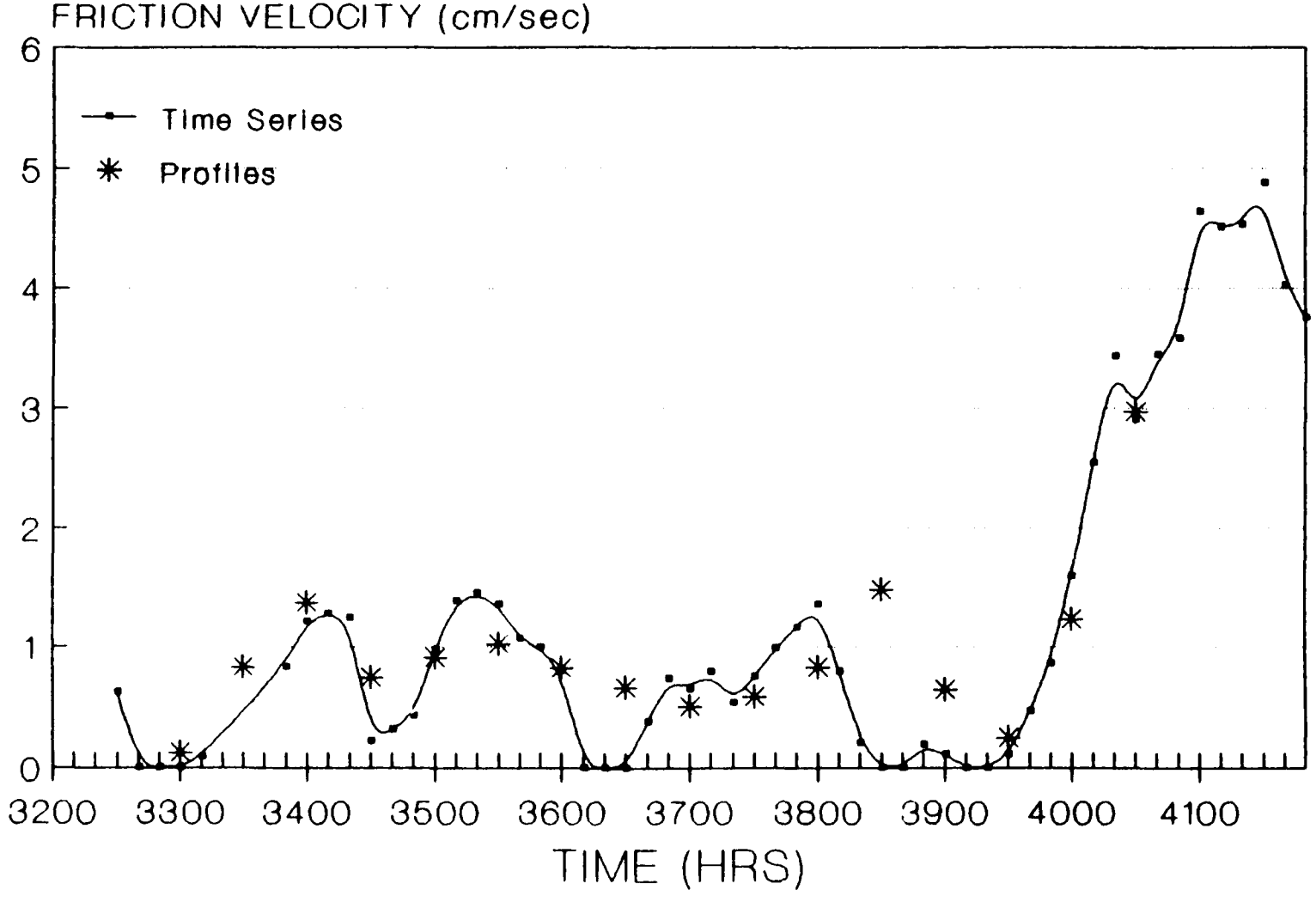

Figure B-3

FRICTION VELOCITY

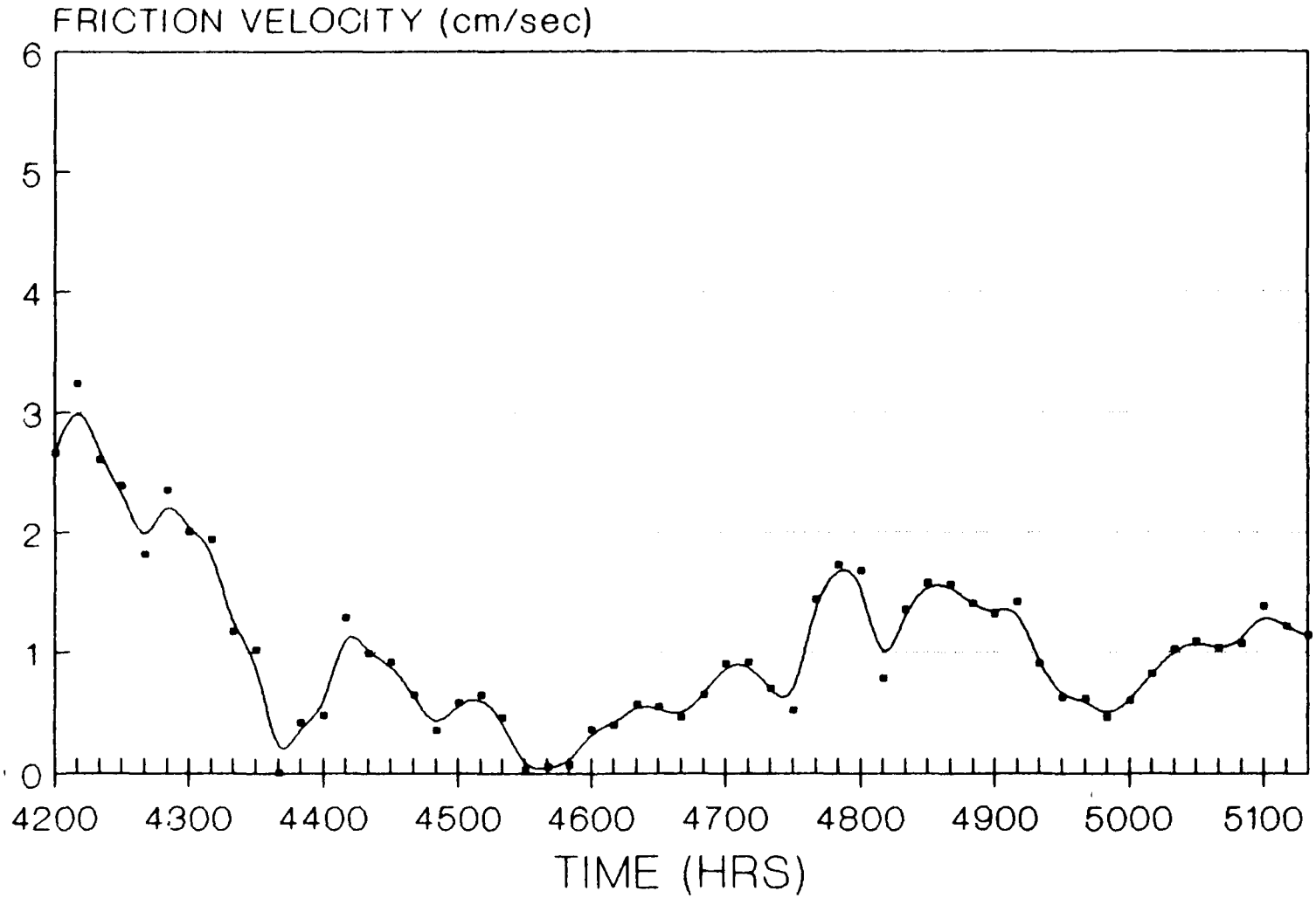

Figure B-4

FRICTION VELOCITY

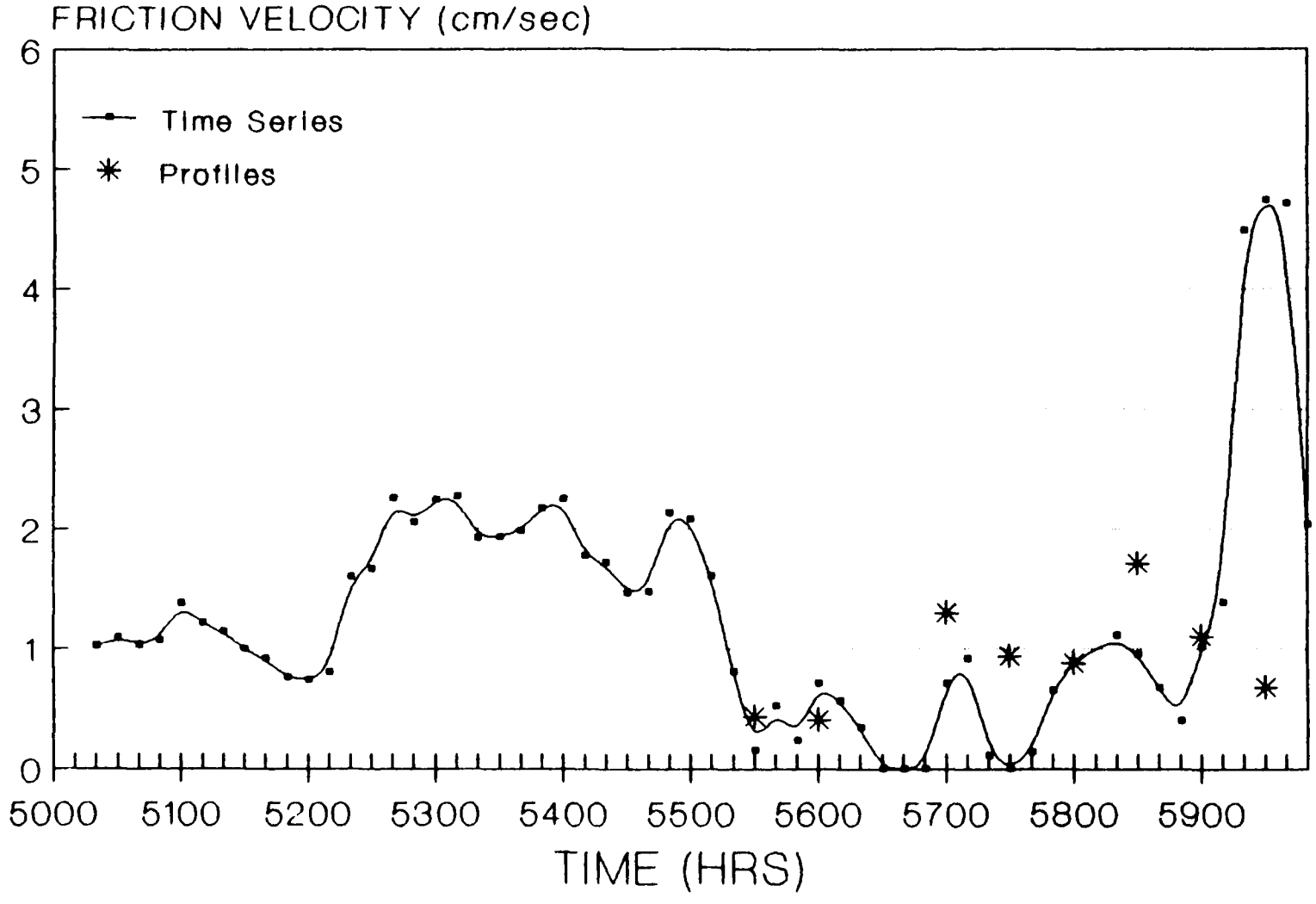

Figure B-5

Appendix C

SUSPENDED SEDIMENT CONCENTRATIONS

This appendix contains a graphical presentation of the suspended sediment concentration time series data (Figures C-1 through C-5). The data presented are that of five scalar concentration values measured at the indicated heights (13, 21, 34, 58, and 87 cm) above the z-datum. Frequently, the sensors at the 13 and 21 cm levels were outside their operating range; therefore, these points are only shown during the times of operation.

The time scale runs continuously from Figure A-1 through Figure A-5 in Appendix A. The time 0000 hours on Figure A-1 is midnight at the beginning of the first day of the measurements. The time 5500 hours on Figure A-5 (for example) is 55 hours later (i.e., 7:00 a.m. on the third day). The lines shown are smooth curves drawn through the given data points.

Vertical suspended sediment concentration distributions for the profile data can be obtained by using Equation 6 in the main text of this report, with the reference concentration and settling velocity data presented in Appendix D and the friction velocity data presented in Appendix B.

SUSPENDED SEDIMENT CONCENTRATION

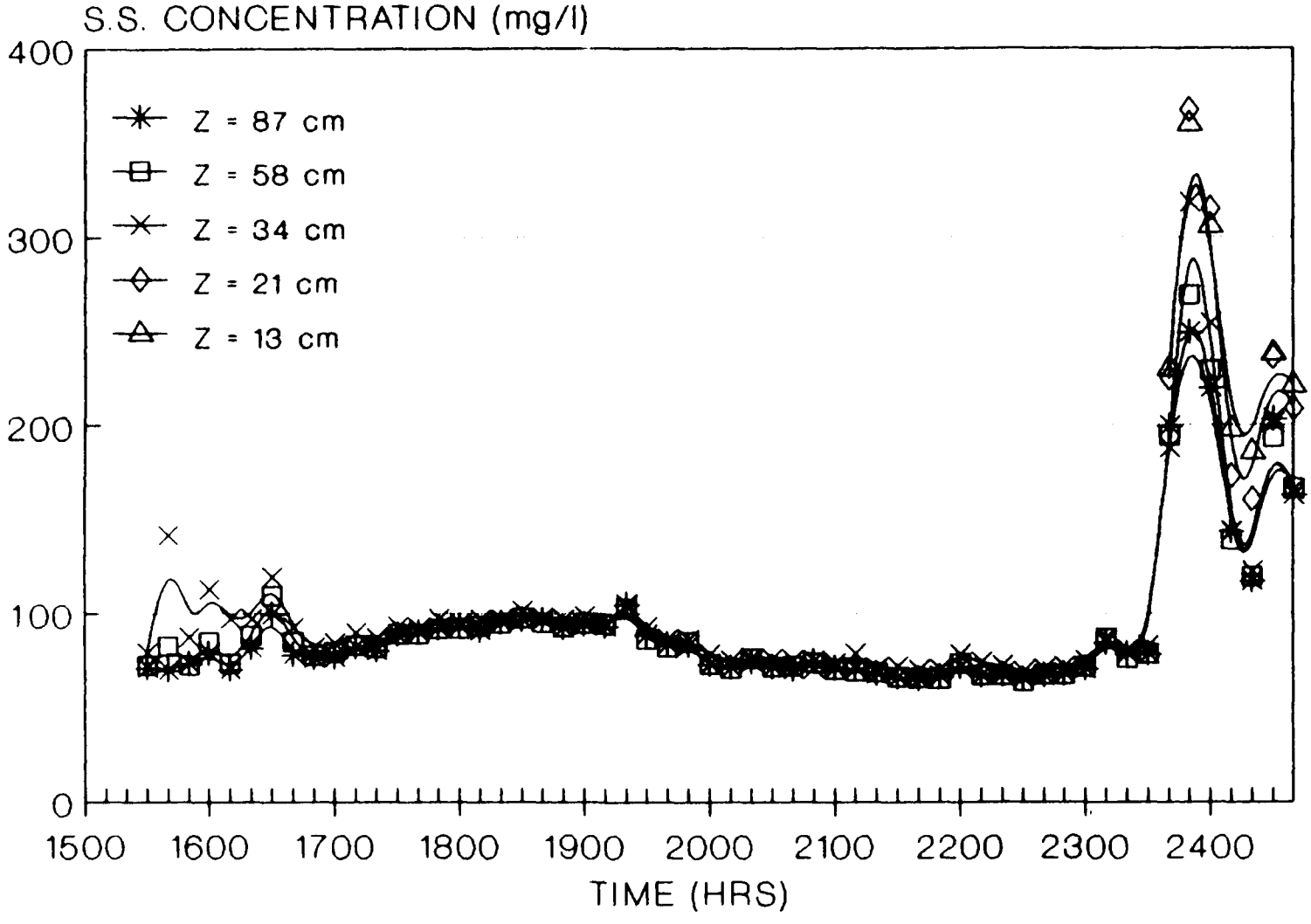

Figure C-1

SUSPENDED SEDIMENT CONCENTRATION

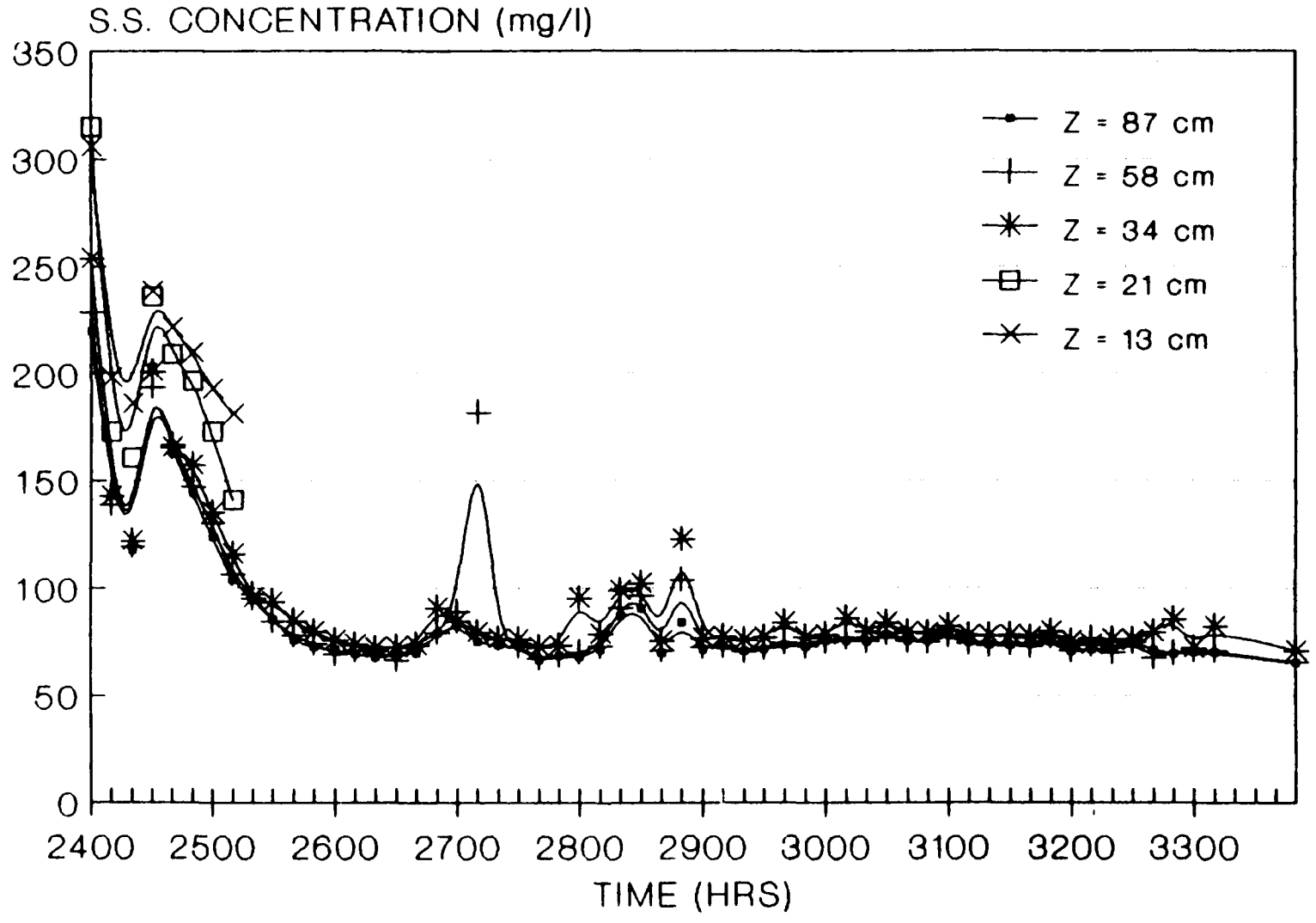

Figure C-2

SUSPENDED SEDIMENT CONCENTRATION

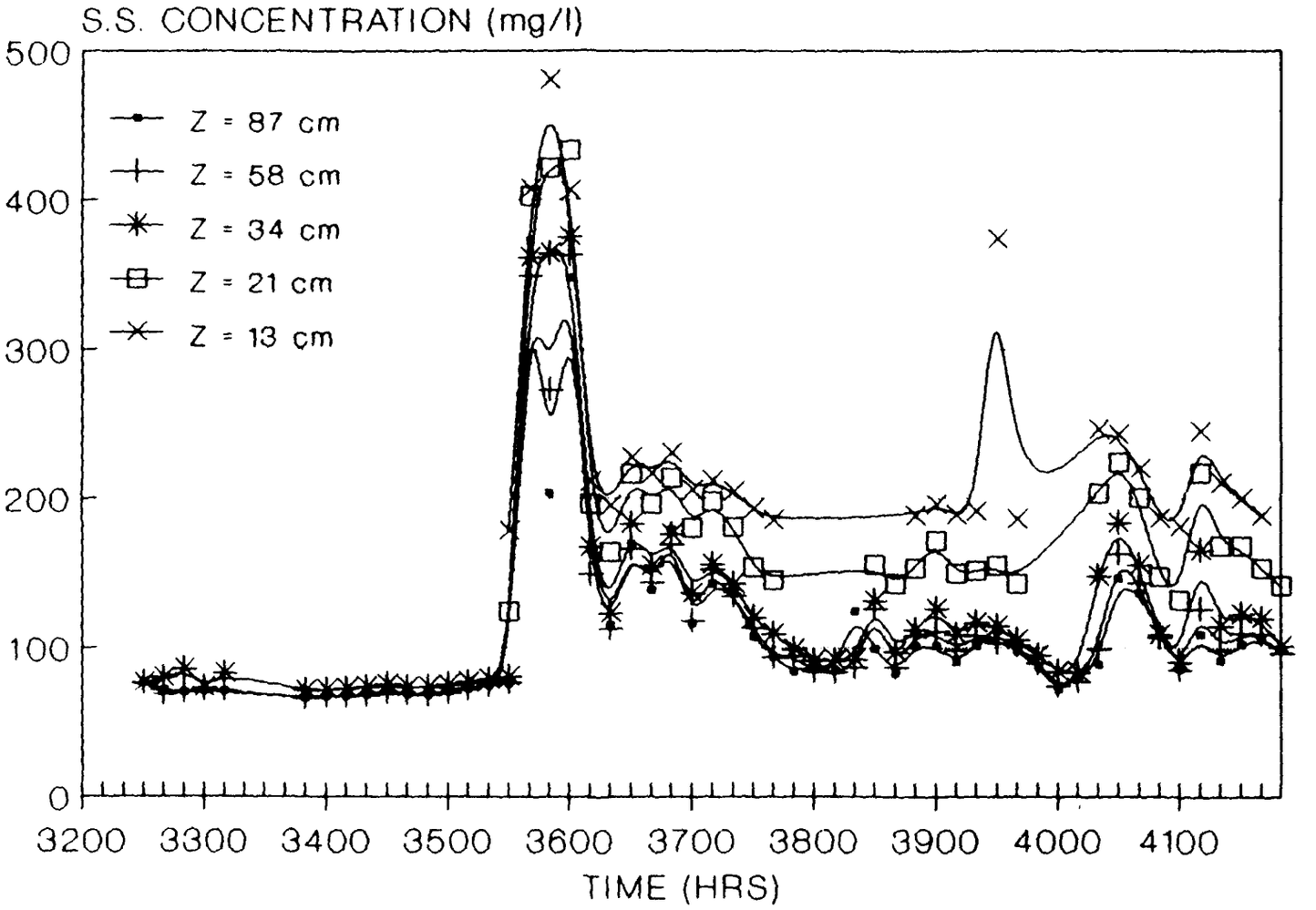

Figure C-3

SUSPENDED SEDIMENT CONCENTRATION

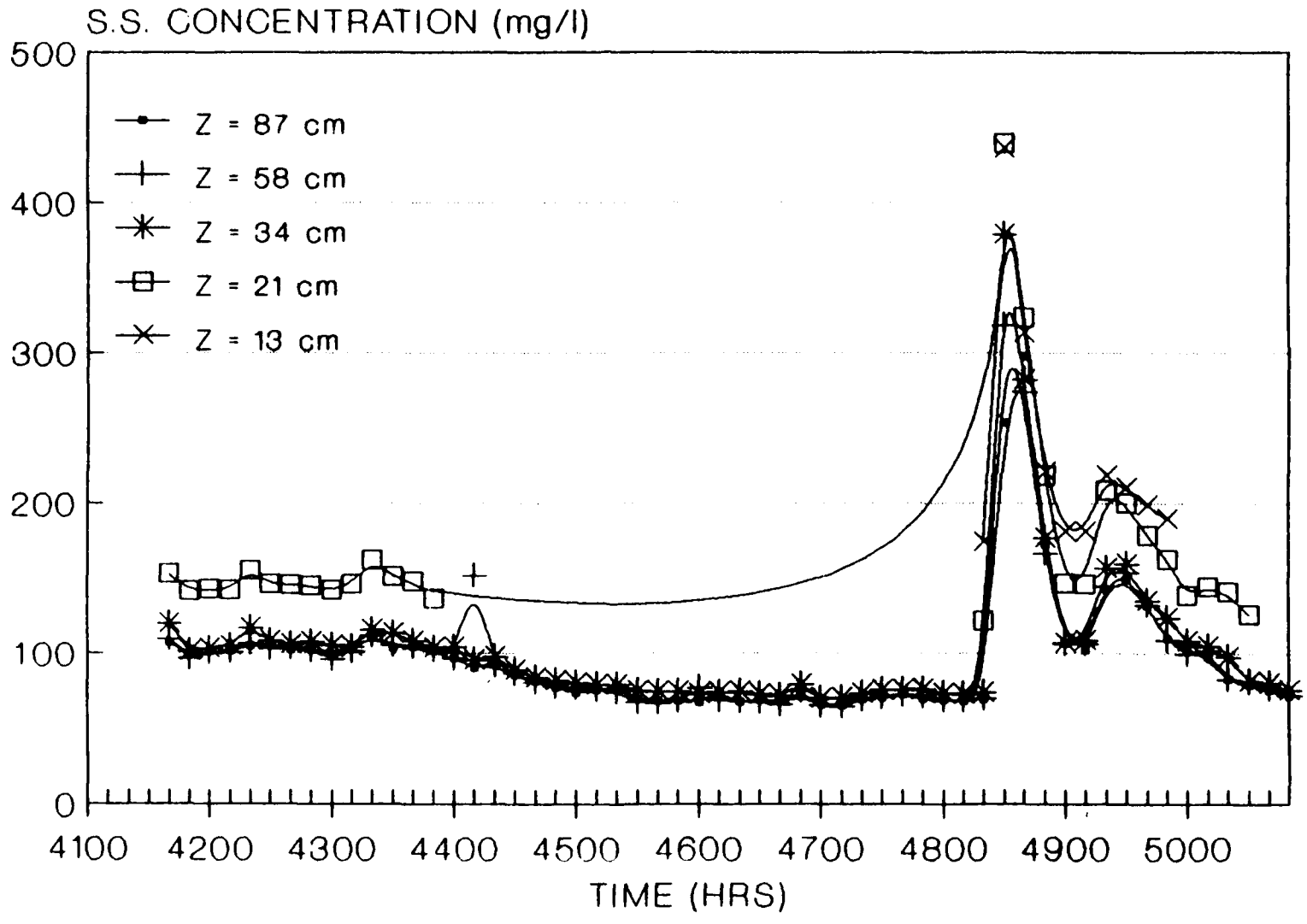

Figure C-4

SUSPENDED SEDIMENT CONCENTRATION

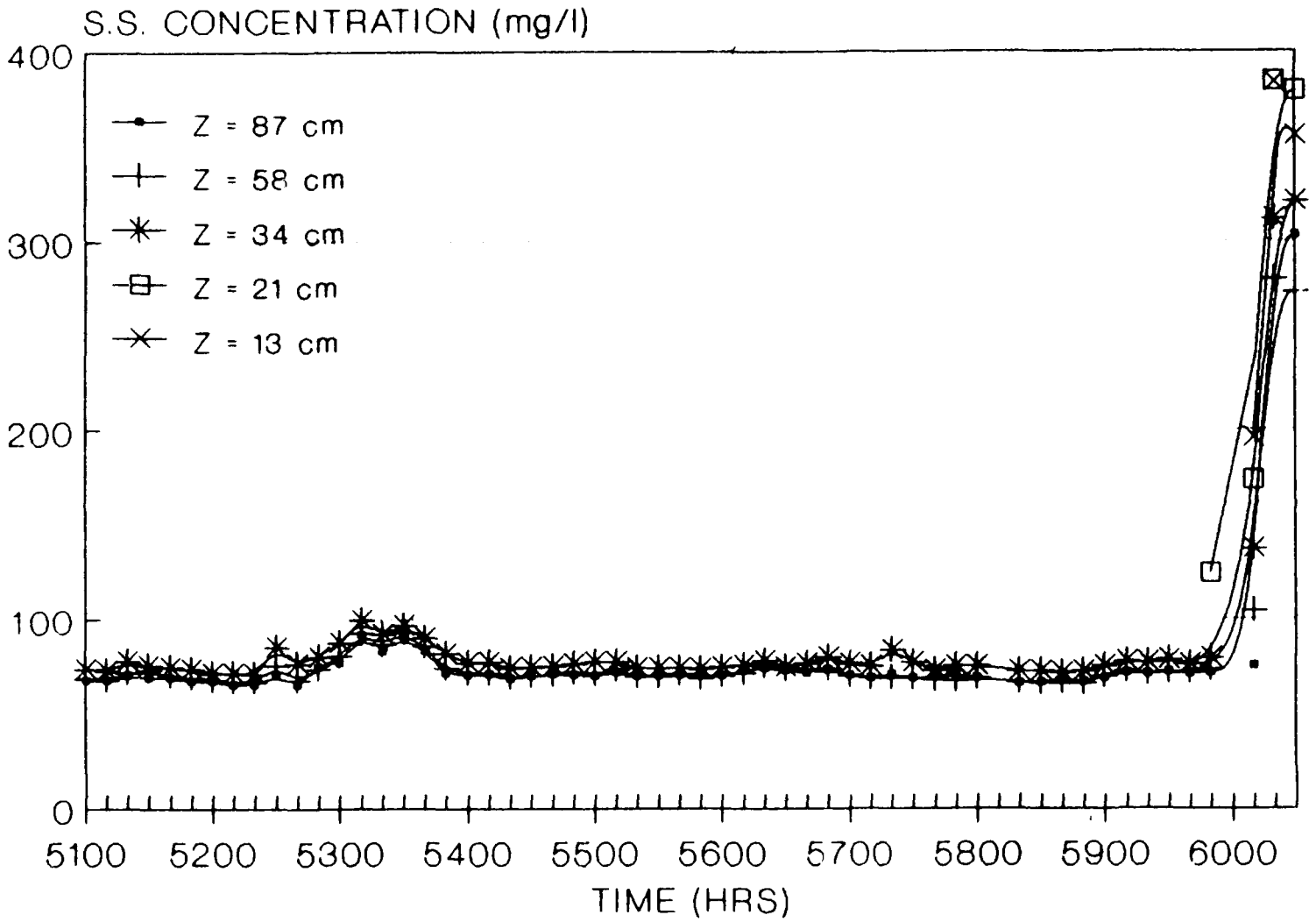

Figure C-5

Appendix D

APPARENT SETTLING VELOCITY

This appendix contains a graphical presentation of the time series and profile settling velocity data (Figures D-1 through D-5) as well as a list of the profile data (Table D-1). The profile data list contains both the apparent settling velocity that is based on the measured vertical suspended sediment concentration distribution, and the reference concentration used. The reference concentration is the measured value at 82 cm above the z-datum. Data are not presented for the latter portion of day 268 due to the failure of the concentration sensor at the level z = 34 cm. This failure, combined with the fact that sensors at z = 13 and 21 cm were operating outside of their range, reduced the vertical extent of the profile sufficiently to render it useless.

The settling velocity time series was computed, using Equation 6 in the main text of this report, from the suspended sediment concentration data presented in Appendix C. The time scale runs continuously from Figure A-1 through Figure A-5 in Appendix A. The time 0000 hours on Figure A-1 is midnight at the beginning of the first day of the measurements. The time 5500 hours on Figure A-5 (for example) is 55 hours later (i.e., 7:00 a.m. on the third day). The line shown in the graphical presentation is a smooth curve drawn through the given data points.

Table D-1. PROFILE DATA

PROFILE DATA

TABLE OF SETTLING VELOCITIES AND REFERENCE CONCENTRATIONS

PROFILE (day-hr)	SETTLING VELOCITY (cm/sec)	REFERENCE CONCENTRATION (mg/l)
266-1530	.067	68.4
266-1600	.069	81.1
266-1630	.163	116.3
266-1700	.039	73.2
266-1730	.001	87.1
266-1800	.026	94.9
267-0700	.016	75.7
267-0730	.012	73.9
267-0830	.016	71.9
267-0900	.003	69.1
267-0930	.024	64.7
267-1000	.034	68.4
267-1030	.020	69.6
267-1100	.031	72.5
267-1130	.014	77.5
267-1200	.058	227.9
267-1230	.069	145.9
267-1300	.048	144.2
267-1330	.011	97.1
267-1400	.009	84.5
267-1430	.052	92.9
267-1500	.056	126.5
267-1530	.027	106.3
267-1600	.275	74.3
267-1630	.337	114.2
268-0730	.011	73.5
268-0800	.003	69.6

APPARENT
SETTLING VELOCITY

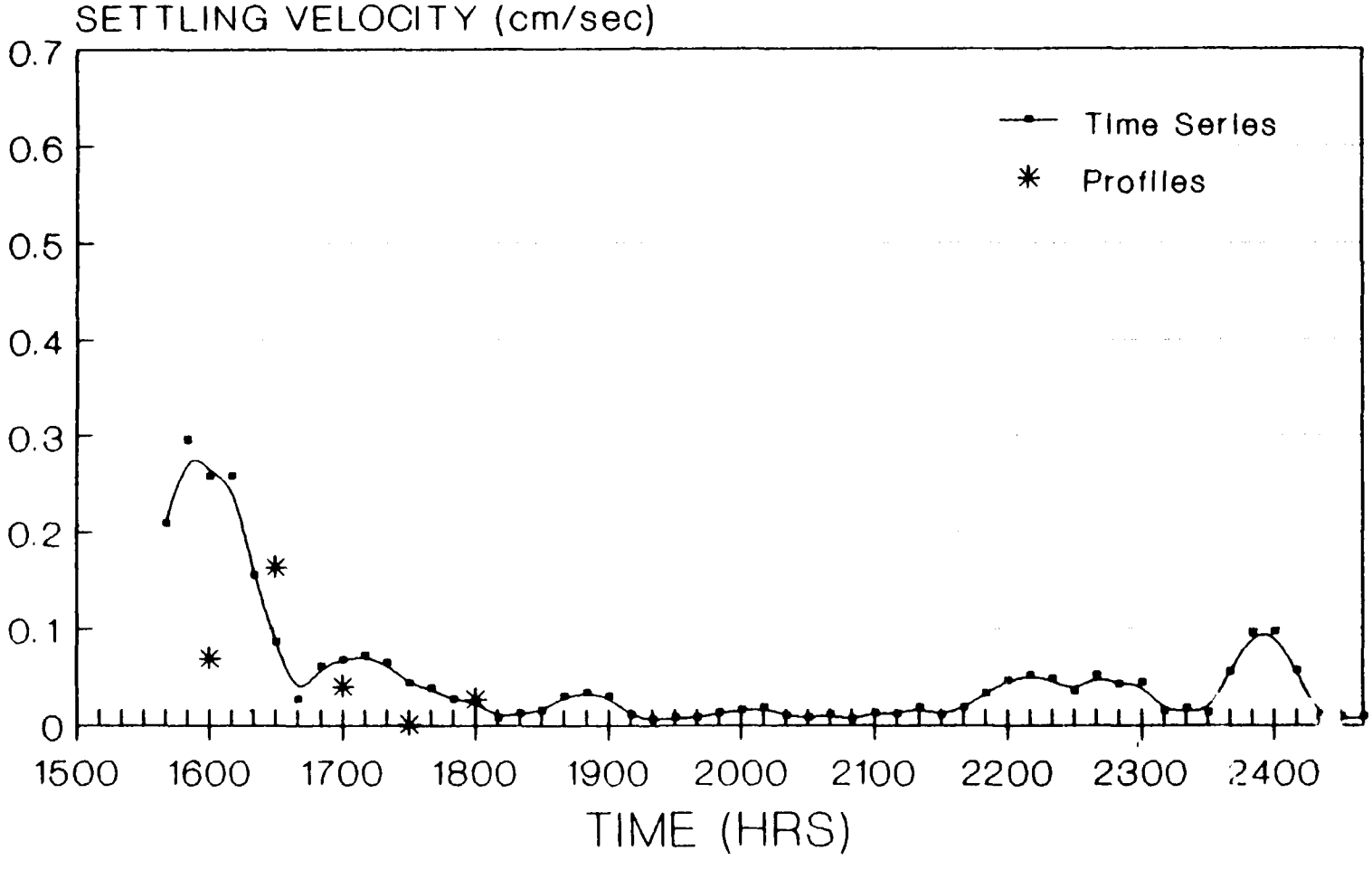

Figure D-1

APPARENT SETTLING VELOCITY

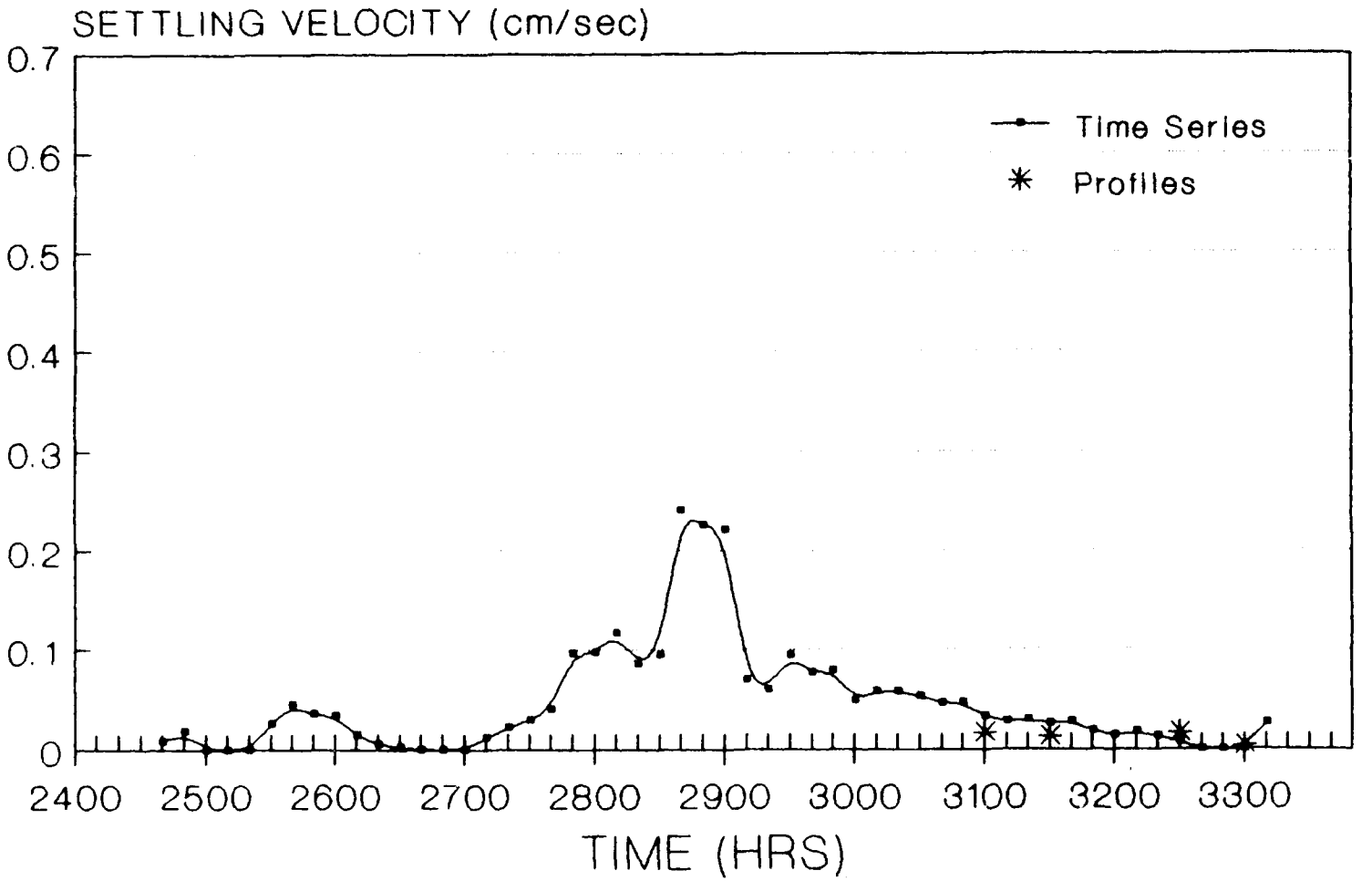

Figure D-2

APPARENT SETTLING VELOCITY

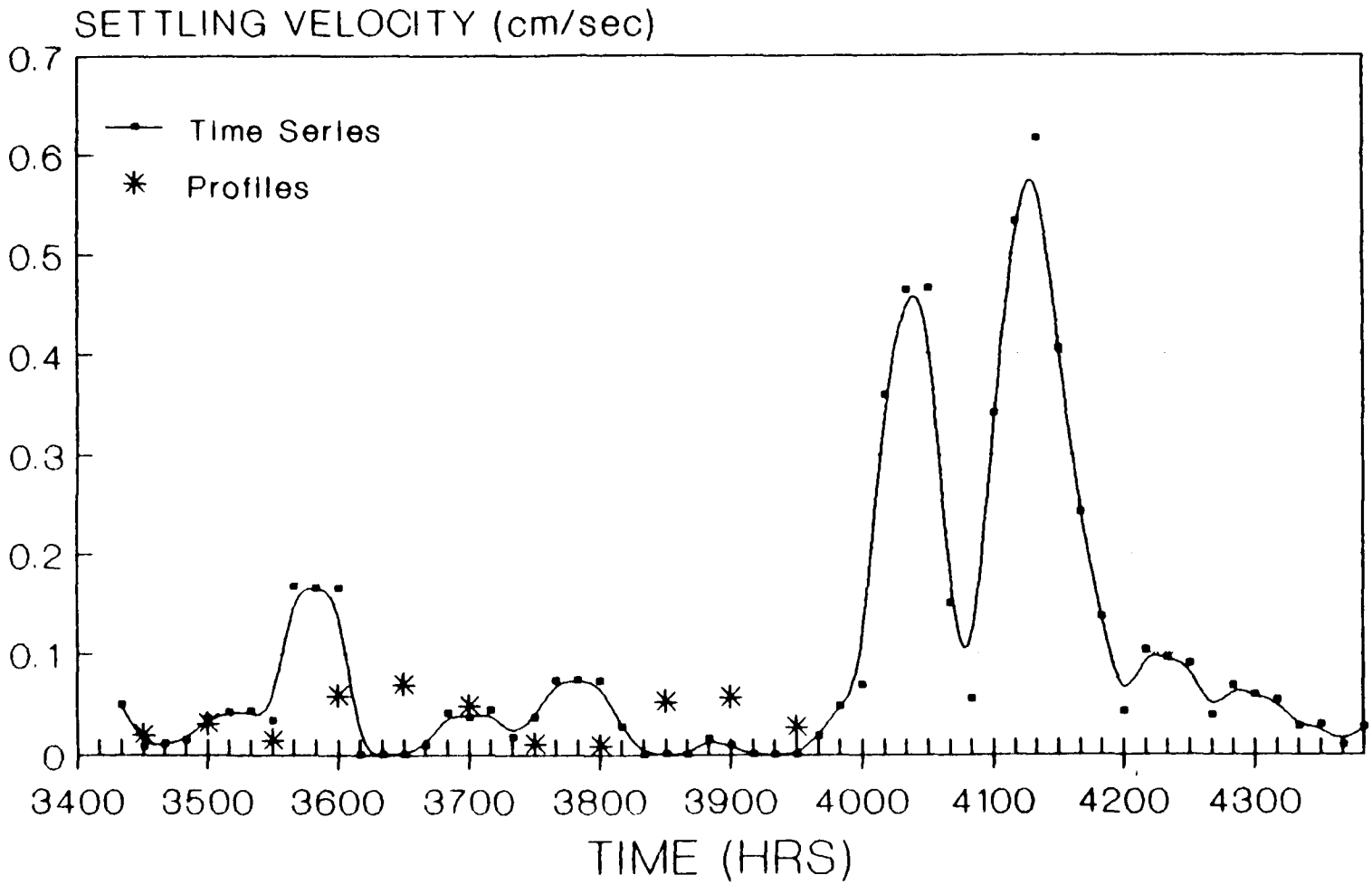

Figure D-3

APPARENT SETTLING VELOCITY

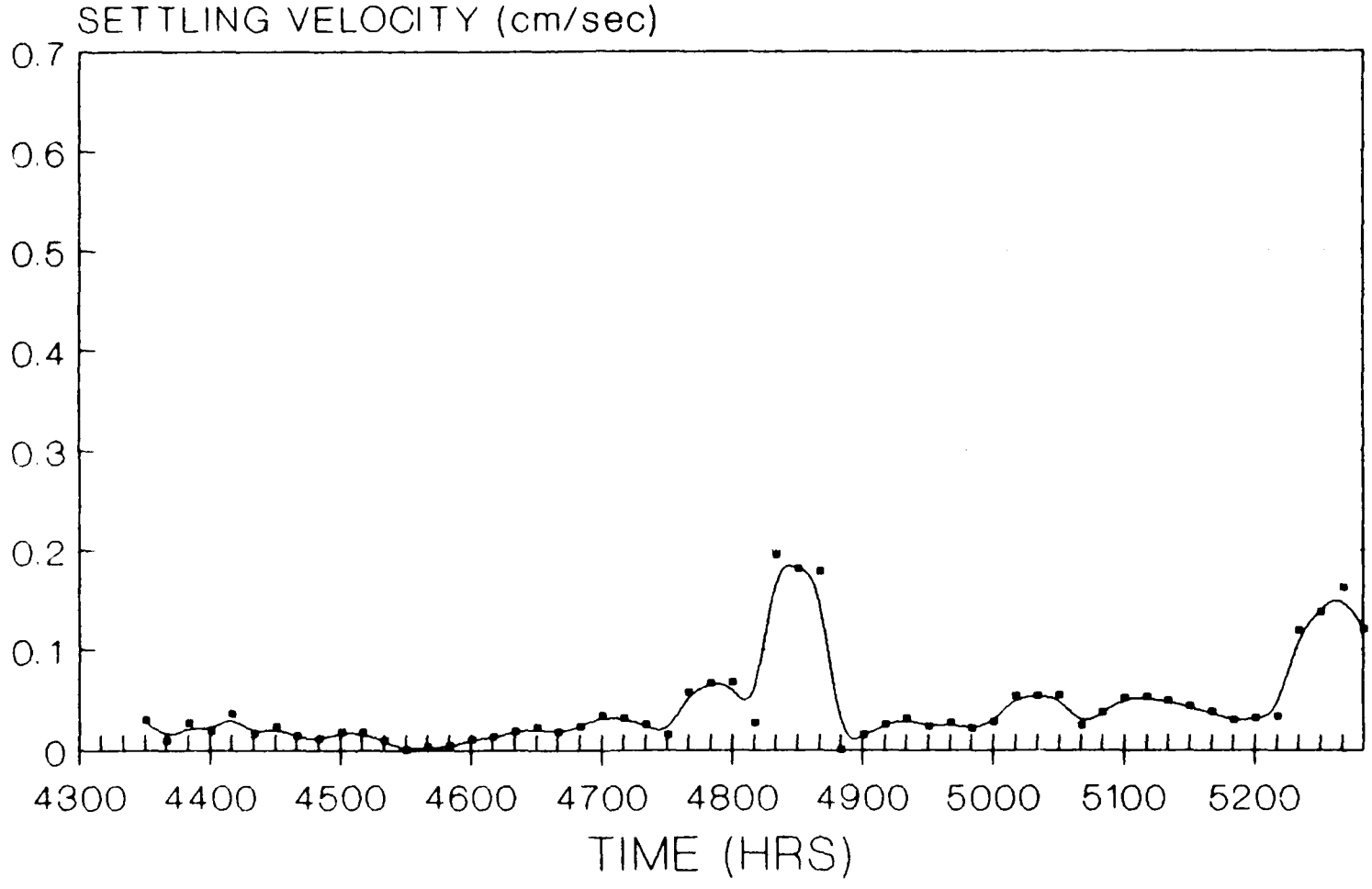

Figure D-4

APPARENT SETTLING VELOCITY

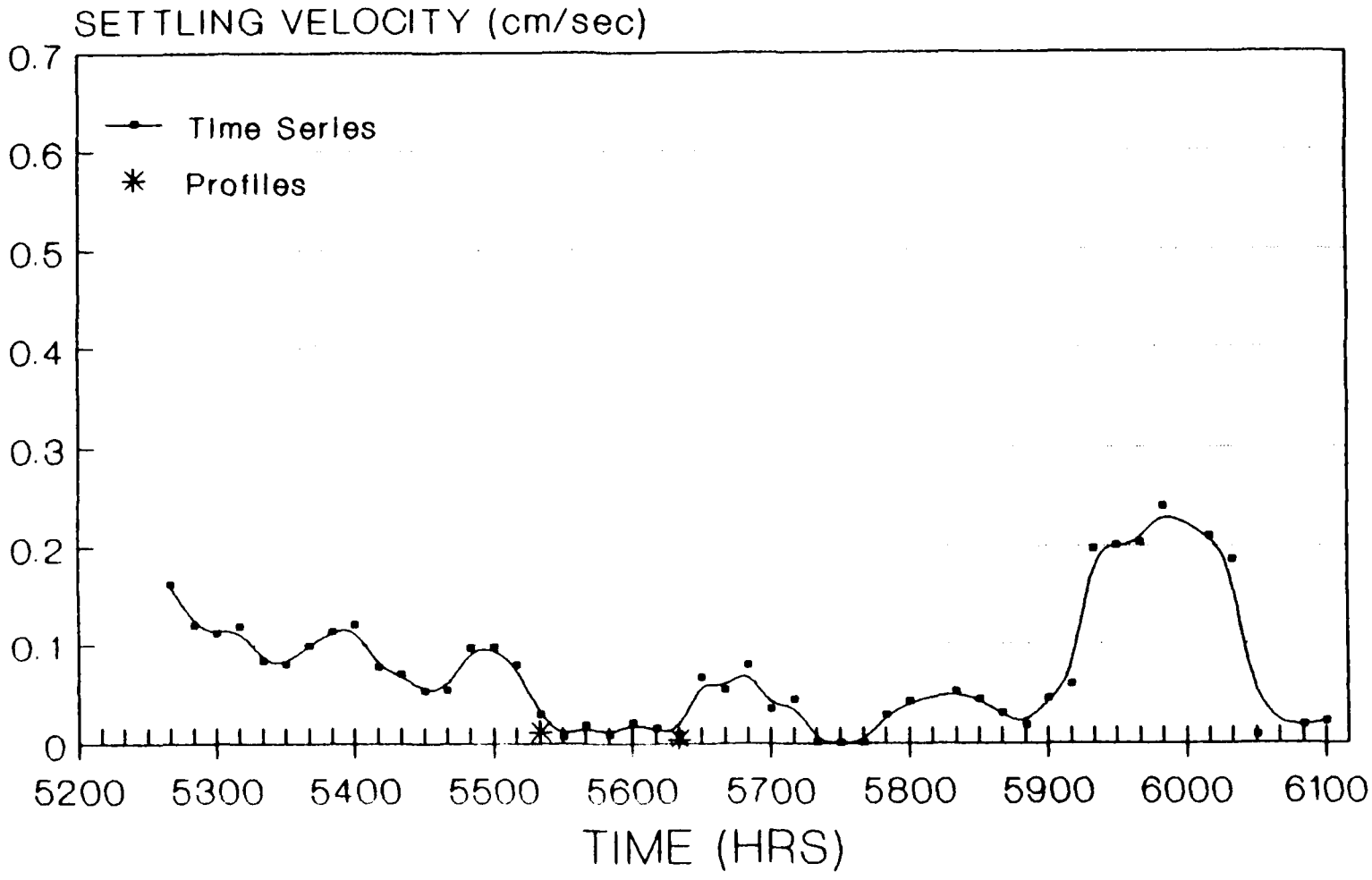

Figure D-5

DISTRIBUTION LIST

AFESC / TIC Lib, Tyndall AFB, FL
ARMY CRREL / CRREL-EA (Kovacs), Hanover, NH
ARMY EWES / Lib, Vicksburg, MS
BATTELLE / New Eng Marine Rsch Lab, Duxbury, MA
CATHOLIC UNIV / CE Dept (Kim) Washington, DC
CNA / Tech Lib, Alexandria, VA
CNO / DCNO, Logs, OP-424C, Washington, DC
CORNELL UNIV / Lib, Ithaca, NY
DIRSSP / Code PM-1, Washington, DC
DTIC / Alexandria, VA
DTRCEN / Code 4120, Annapolis, MD
DUKE UNIV / CE Dept (Muga), Durham, NC
EG7G WASH ANAL. SVC CEN / Bonde, Gaithersburg, MD
FLORIDA ATLANTIC UNIV / Ocean Engrg Dept (McAllister), Boca Raton, FL
FLORIDA ATLANTIC UNIV / Ocean Engrg Dept (Su), Boca Raton, FL
FLORIDA INST OF TECH / CE Dept (Kalajian), Melbourne, FL
GEORGIA INST OF TECH / CE Schl (Mazanti), Atlanta, GA
GIDEP / OIC, Corona, CA
INST OF MARINE SCIENCES / Dir, Morehead City, NC
INST OF MARINE SCIENCES / Lib, Port Aransas, TX
IOWA STATE UNIV / CE DEPT (Handy), Ames, IA
LAMONT-DOHERTY GEOL OBSERVATORY / McCoy, Palisades, NY
LEHIGH UNIV / Linderman Library, Bethlehem, PA
LEHIGH UNIV / Marine Geotech Lab, Bethleham, PA
LIBRARY OF CONGRESS / Sci & Tech Div, Washington, DC
LINDA HALL LIBRARY / Doc Dept, Kansas City, MO
MAINE MARITIME ACADEMY / Lib, Castine, ME
MARITIME ADMIN / MAR-770, Washington, DC
MARITIME ADMIN / MMA, Lib, Kings Point, NY
MICHIGAN TECH UNIV / CO Dept (Haas), Houghton, MI
MIT / Engrg Lib, Cambridge, MA
MIT / Lib, Tech Reports, Cambridge, MA
NATL ACADEMY OF ENGRY / Alexandria, VA
NATL ACADEMY OF SCIENCES / NRC, Dr. Chung, Washington, DC
NATL ACADEMY OF SCIENCES / NRC, Naval Studies Bd, Washington, DC
NAVAIRENGCEN / Code 1822, Lakehurst, NJ
NAVAL WAR COLLEGE / Code 24, Newport, RI
NAVCOASTSYSCEN / Code 2360, Panama City, FL
NAVCOASTSYSCEN / Tech Lib, Panama City, FL
NAVEODTECHCEN / Tech Lib, Indian Head, MD
NAVFACENGCOM - WESTDIV / Code 04A2.2, San Bruno, CA
NAVFACENGCOM / Code 04A3, Alexandria, VA
NAVFACENGCOM / Code 07A (Herrmann), Alexandria, VA
NAVFACENGCOM / Code 09M124 (Lib), Alexandria, VA
NAVFACENGCOM CHESDIV / FPO-1PL, Washington, DC
NAVFACENGCOM SOUTHDIV / Lib, Charleston, SC
NAVOCEANO / Lib, NSTL, MS
NAVOCEANSYSCEN / Code 94, San Diego, CA
NAVOCEANSYSCEN / DET, Tech Lib, Kailua, HI
NETC / Code 42, Newport, RI

NEW YORK STATE MARITIME COLLEGE / Longobardi, Bronx, NY
NOAA / E-AI216, Seattle, WA
NORDA / Code 410, NSTL, MS
NORDA / Code 440, NSTL, MS
NORTHWESTERN UNIV / CE Dept (Dowding), Evanston, IL
NRL / Code 2511, Washington, DC
NUSC DET / Code TA131, New London, CT
NY CITY COMMUNITY COLLEGE / Lib, Brooklyn, NY
OCNR / Code 1121 (EA Silva), Arlington, VA
OREGON STATE UNIV / Oceanography Scol, Corvallis, OR
PENNSYLVANIA STATE UNIV / Applied Rsch Lab, State College, PA
PURDUE UNIV / Engrg Lib, West Lafayette, IN
PWC / Tech Lib, FPO San Francisco,
SAUDI ARABIA / King Saud Univ, ,
SEATTLE UNIV / CE Dept (Schwaegler), Seattle, WA
STATE UNIV OF NEW YORK / CE Dept, Buffalo, NY
SUPSHIP / Tech Lib, Newport News, VA
TEXAS A&I UNIV / Civil & Mech Engr Dept (Parate), Kingsville, TX
TEXAS A&M UNIV / CE Dept (Herbich), College Station, TX
TEXAS A&M UNIV / Ocean Engr Proj, College Station, TX
TEXAS TECH UNIV / IE Dept (Ayoub), Lubbock, TX
UNITED KINGDOM / Inst of Oceanographic Sci, Wormely, Godalming,, Surrey
UNIV OF ALASKA / Biomed & Marine Sci Lib, Fairbanks, AK
UNIV OF CONNECTICUT / Lib, Groton, CT
UNIV OF HARTFORD / CE Dept (Keshawarz), West Hartford, CT
UNIV OF HAWAII / Manoa, Lib, Honolulu, HI
UNIV OF ILLINOIS / Lib, Urbana, IL
UNIV OF ILLINOIS / Metz Ref Rm, Urbana, IL
UNIV OF MICHIGAN / CE Dept (Richart), Ann Arbor, MI
UNIV OF NEW HAMPSHIRE / Diving Safety Office, Durham, NH
UNIV OF RHODE ISLAND / CE Dept (Kovacs), Kingston, RI
UNIV OF SO CALIFORNIA / Hancock Lib, Los Angeles, CA
UNIV OF TEXAS / CE Dept (R. Olson), Austin, TX
UNIV OF WASHINGTON / RL Terrel, Edmonds, WA
UNIV OF WISCONSIN / Great Lakes Studies Cen, Milwaukee, WI
US ARMY ENGRSCHOOL / ATSE-DAC-LB, Fort Leonard Wood, MO
US GEOLOGICAL SURVEY / J Bales, Raleigh, NC
US GEOLOGICAL SURVEY / Marine Geological Offc, Reston, VA
USNA / PWO, Annapolis, MD
VIRGINIA INST OF MARINE SCI / Lib, Gloucester Point, VA
VSE / Ocean Engrg Gp (Murton), Alexandria, VA
WORCESTER POLYTECH INST / J.M. Sullivan, Worcester, MA

INSTRUCTIONS

The Naval Civil Engineering Laboratory has revised its primary distribution lists. The bottom of the label on the reverse side has several numbers listed. These numbers correspond to numbers assigned to the list of Subject Categories. Numbers on the label corresponding to those on the list indicate the subject category and type of documents you are presently receiving. If you are satisfied, throw this card away (or file it for later reference).

If you want to change what you are presently receiving:

- Delete - mark off number on bottom of label.
- Add - circle number on list.
- Remove my name from all your lists - check box on list.
- Change my address - line out incorrect line and write in correction **(DO NOT REMOVE LABEL)**.
- Number of copies should be entered after the title of the subject categories you select.

Fold on line below and drop in the mail.

Note: Numbers on label but not listed on questionnaire are for NCEL use only, please ignore them.

Fold on line and staple.

DEPARTMENT OF THE NAVY

Naval Civil Engineering Laboratory
Port Hueneme, CA 93043-5003

Official Business
Penalty for Private Use, $300

NO POSTAGE
NECESSARY
IF MAILED
IN THE
UNITED STATES

BUSINESS REPLY CARD

FIRST CLASS PERMIT NO. 12503 WASH D.C.

POSTAGE WILL BE PAID BY ADDRESSEE

Commanding Officer
Code L34
Naval Civil Engineering Laboratory
Port Hueneme, California 93043-5003

DISTRIBUTION QUESTIONNAIRE

The Naval Civil Engineering Laboratory is revising its Primary distribution lists.

SUBJECT CATEGORIES

1 SHORE FACILITIES
2 Construction methods and materials (including corrosion control, coatings)
3 Waterfront structures (maintenance/deterioration control)
4 Utilities (including power conditioning)
5 Explosives safety
6 Aviation Engineering Test Facilities
7 Fire prevention and control
8 Antenna technology
9 Structural analysis and design (including numerical and computer techniques)
10 Protective construction (including hardened shelters, shock and vibration studies)
11 Soil/rock mechanics
14 Airfields and pavements

15 ADVANCED BASE AND AMPHIBIOUS FACILITIES
16 Base facilities (including shelters, power generation, water supplies)
17 Expedient roads/airfields/bridges
18 Amphibious operations (including breakwaters, wave forces)
19 Over-the-Beach operations (including containerization, material transfer, lighterage and cranes)
20 POL storage, transfer and distribution

28 ENERGY/POWER GENERATION
29 Thermal conservation (thermal engineering of buildings, HVAC systems, energy loss measurement, power generation)
30 Controls and electrical conservation (electrical systems, energy monitoring and control systems)
31 Fuel flexibility (liquid fuels, coal utilization, energy from solid waste)
32 Alternate energy source (geothermal power, photovoltaic power systems, solar systems, wind systems, energy storage systems)
33 Site data and systems integration (energy resource data, energy consumption data, integrating energy systems)
34 ENVIRONMENTAL PROTECTION
35 Hazardous waste minimization
36 Restoration of installations (hazardous waste)
37 Waste water management and sanitary engineering
38 Oil pollution removal and recovery
39 Air pollution

44 OCEAN ENGINEERING
45 Seafloor soils and foundations
46 Seafloor construction systems and operations (including diver and manipulator tools)
47 Undersea structures and materials
48 Anchors and moorings
49 Undersea power systems, electromechanical cables, and connectors
50 Pressure vessel facilities
51 Physical environment (including site surveying)
52 Ocean-based concrete structures
54 Undersea cable dynamics

TYPES OF DOCUMENTS

85 Techdata Sheets 86 Technical Reports and Technical Notes
83 Table of Contents & Index to TDS
82 NCEL Guides & Abstracts
91 Physical Security

☐ None-remove my name

NCEL DOCUMENT EVALUATION

You are number one with us; how do we rate with you?

We at NCEL want to provide you our customer the best possible reports but we need your help. Therefore, I ask you to please take the time from your busy schedule to fill out this questionnaire. Your response will assist us in providing the best reports possible for our users. I wish to thank you in advance for your assistance. I assure you that the information you provide will help us to be more responsive to your future needs.

R. N. STORER, Ph.D, P.E.
Technical Director

DOCUMENT NO. _____ TITLE OF DOCUMENT: _____

_____

Date: _____ Respondent Organization : _____

Name: _____ Activity Code: _____
Phone: _____ _____ Grade/Rank: _____

Category (*please check*):

Sponsor ____ User ____ Proponent ____ Other (*Specify*) _____

Please answer on your behalf only; not on your organization's. Please check (*use an X*) only the block that most closely describes your attitude or feeling toward that statement:

SA Strongly Agree A Agree O Neutral D Disagree SD Strongly Disagree

---

	SA	A	N	D	SD
1. The technical quality of the report is comparable to most of my other sources of technical information.	( )	( )	( )	( )	( )
2. The report will make significant improvements in the cost and or performance of my operation.	( )	( )	( )	( )	( )
3. The report acknowledges related work accomplished by others.	( )	( )	( )	( )	( )
4. The report is well formatted.	( )	( )	( )	( )	( )
5. The report is clearly written.	( )	( )	( )	( )	( )
6. The conclusions and recommendations are clear and directly supported by the contents of the report.	( )	( )	( )	( )	( )
7. The graphics, tables, and photographs are well done.	( )	( )	( )	( )	( )

Do you wish to continue getting NCEL reports? ☐ YES ☐ NO

Please add any comments (e.g., in what ways can we improve the quality of our reports?) on the back of this form.

Comments:

Please fold on line and staple

DEPARTMENT OF THE NAVY

Naval Civil Engineering Laboratory
Port Hueneme, CA 93043-5003

Official Business
Penalty for Private Use $300

Code L03B
NAVAL CIVIL ENGINEERING LABORATORY
PORT HUENEME, CA 93043-5003